LA-UR-20-24561
Approved for public release; distribution is unlimited.

Title: Beryllium Oxide (BeO) Handbook

Author(s): PETROVIC, J. J.
Haertling, Carol Lynn

Intended for: Report

Issued: 2020-06-24

Beryllium Oxide (BeO) Handbook

Los Alamos National Laboratory
Los Alamos, NM 87545

May 2020
John Petrovic (retired)

1. General

Beryllium oxide (BeO) is an oxide ceramic material. BeO ceramics provide thermal conductivity second only to diamond among electrically insulating materials, dissipating nearly 300 W/mK at room temperature. This property leads to electronic applications for BeO.

BeO has a thermal expansion coefficient intermediate between gallium arsenide and refractory metal composites. Its low dielectric constant (6.7) and low loss index (0.0012 at 1 MHz) permits electrical circuit performance at high frequencies. It is employed as a window material for high frequency microwave applications.

BeO is very stable under oxidizing and reducing high temperature and high humidity environments, unlike nitrides which will decompose to their oxide equivalent.

Similar to beryllium metal, BeO acts as a scatterer of neutrons and is used as a neutron moderator material in nuclear reactor applications.

The largest use of BeO is as the raw material for the manufacture of beryllium-copper alloys, followed closely as the raw material for conversion to beryllium metal.

Most of the research performed on BeO was conducted in the 1960's and 1970's. 75% of the references cited in this Handbook are from the time period 1960-1980.

Up to 1995, there were three commercial sources of BeO: Materion Corporation, Eagle-Picher, and Ceradyne Corporation. However, since 1995 Eagle-Picher and Ceradyne no longer supply BeO commercial products. Thus, the only current commercial source of BeO materials is Materion Corporation.

1.01 Commercial Designations

1.011 Materion Corporation:

Materion Corporation (6100 S. Tucson Blvd., Tucson, Arizona 85706) is currently the only U.S. commercial source of BeO products. Materion's BeO manufacturing capabilities include dry pressing, isopressing, extruding, sintering, diamond machining, and laser drilling.

The standard Materion BeO material is Isopressed Thermalox 995.

1.02 Commercial Specifications

1.021 Materion Corporation:

The commercial specifications for Materion Isopressed Thermalox 995 BeO are shown in Figure 1.021.

1.03 Composition

1.031 Materion Corporation:

The composition of Materion Isopressed Thermalox 995 BeO is shown in Figure 1.021. The BeO content is 99.5% minimum.

1.04 Forms and Conditions Available

1.041 Materion Corporation:

Materion Isopressed Thermalox 995 BeO is available as tubes, rods, bars, plate, and blocks (see Figure 1.021).

1.05 Special Considerations

1.051 Health hazards:

The health hazards with BeO are similar to those of beryllium (1). Beryllium exposure can cause Chronic Beryllium Disease (CBD) in those people who are genetically hypersensitive to beryllium. CBD is a lung disease that, once acquired, is incurable, and which has an approximately 30% fatality rate. The incidence of CBD in beryllium machinists has averaged about 15%. If one is in the 85% of the population that is not genetically hypersensitive to beryllium, then there is essentially no problem with beryllium or beryllium oxide exposure. However, if one belongs to the 15% of the population that is hypersensitive to beryllium, a significant health hazard may exist if exposed, even in a minor way, to beryllium or beryllium oxide. It has been reported that secretaries at some beryllium plants acquired CBD, even though they never went into the beryllium operational areas. Genetic tests are currently under development to determine genetic hypersensitivity of individuals to beryllium and beryllium oxide (2).

1.052 Exposure limits:

The current DOE exposure limit for airborne beryllium or BeO particles is 0.2 $\mu g/m^3$ for an eight hour time-weighted average (3).

2. Physical and Chemical Properties

2.01 Thermal Properties

2.011 Melting point:

The melting point of BeO is 2570 ºC (4).

2.012 Phase changes:

There is only one phase change in cooling BeO down from its melting point. From the melting point of 2570 ºC to 2049 ºC, BeO exists in a tetragonal β-BeO crystal structure. Below 2049 ºC, the crystal structure of BeO is the hexagonal α-BeO form (4).

2.013 Thermal conductivity:

The thermal conductivity of BeO as a function of temperature and % theoretical density (4) is shown in Figure 2.013.

2.014 Thermal expansion:

The thermal expansion of BeO as a function of temperature (4) is shown in Figure 2.014.

2.015 Specific heat:

The specific heat of BeO as a function of temperature (4) is shown in Figure 2.015.

2.02 Other Physical Properties

2.021 Density:

The theoretical density of hexagonal BeO is 3.008 g/cm^3 (4). The theoretical density of tetragonal BeO is 2.69 g/cm^3.

2.022 Electrical properties:

2.0221 Electrical conductivity:

The electrical conductivity of BeO as a function of temperature (5) is shown in Figure 2.0221. BeO is a hard insulator at room temperature.

2.0222 Dielectric constant:

The dielectric constant of BeO at room temperature (6) is reported to have a value of 6.3. BeO is considered to be a low dielectric constant material.

2.03 Chemical Properties

2.031 Vapor pressure:

The vapor pressure of BeO as a function of temperature is given by the following expression (7):

$\text{Log } P_{BeO} \text{ (mm Hg)} = (18.015) - (1.77)(\log T) - (38247)(T^{-1})$ (for 298 – 2500 °K)

It should be noted that at 2300 °K, the vapor above BeO consists of Be, O, BeO, $(BeO)_2$, $(BeO)_3$, $(BeO)_4$, $(BeO)_5$, $(BeO)_6$, Be_2O, and other species.

The measured vapor pressure of BeO (91) from 2100-2570 °K is shown in Figure 2.031. It is in the range of 10^{-5} atm at 2570 °K to 10^{-8} atm at 2100 °K

2.032 Oxidation resistance:

Since BeO is an oxide material, it possesses superb oxidation resistance.

2.033 Corrosion resistance:

2.0331 Water and water vapor:

At high temperatures, BeO reacts with water vapor to form a gaseous product according to the following reaction (8):

$$BeO\ (s) + H_2O\ (g) = Be(OH)_2\ (g)$$

The reaction with water causes a weight loss due to the volatilization of $Be(OH)_2$, which then decomposes upon cooling to recondense as BeO.

The loss of weight (W) from a BeO sample depends on its surface area (S), the mass flow rate (M) of water vapor over the sample, and the temperature (T) according to the following empirical expression (4):

$$W = (K)\ (S)\ (M^{0.3})\ (\exp(-6000/RT)$$

As the atmosphere above BeO approaches the saturation concentration of $Be(OH)_2$, the rate of weight loss from BeO decreases until equilibrium is finally attained. Under conditions of equilibrium, the moles of BeO lost (N_{BeO}) with respect to temperature and the moles of water vapor (N_{H2O}) consumed is indicated to be (8):

$$\log (N_{BeO}) = (A) - (B/T) + \log (N_{H2O})$$

where T is given in °K. Reported values of the empirical constants in the expression above are in the ranges A = 1.62-193 and B = 8.8-9.3 x 10^3

2.0332 Molten metals:

Because of its inertness to reactive molten metals, BeO has in the past been used for crucibles and thermocouple protection tubes. BeO is considered the best crucible material for the melting of Be metal.

2.0333 Gases:

At high temperatures, BeO is stable with respect to oxidizing gases, and reducing gases such as hydrogen.

2.04 Nuclear Properties

2.041 Neutronics

The neutronics of BeO are similar to the neutronics of Be (9). BeO acts predominantly as a scatterer of neutrons, changing their direction and reducing their energy. Because of this, it is a high temperature moderator material for nuclear fission reactors.

2.05 Thermodynamic Properties

The thermodynamic properties of importance are the heat capacity at constant pressure C_p , the enthalpy H, the entropy S, and the Gibbs free energy G. These thermodynamic properties are defined as follows:

$$C_p = (dH/dT)_p$$

$$H(T) = H_f(298) + \int_{298}^{T} C_p \, dT + \sum H_{tr}$$

$$S = S_o(298) + \int_{298}^{T} (C_p/T)dT + \sum H_{tr}/T_{tr}$$

$$G = H - TS$$

T is the temperature in °K. $H_f(298)$ is the enthalpy of formation at 298 °K. H_{tr} is the enthalpy of transformation of the substance. H = 0 for the elements in their most stable state at 298 °K and 1 atmosphere pressure. The enthalpy of compounds also contains their enthalpy of formation ΔH_f from elements. $S_o(298)$ is the standard entropy of a substance.

Figures 2.051-2.054 show these thermodynamic quantitities for BeO (90, 92-96).

Another thermodynamic aspect of interest is the Ellingham diagram, which compares the stability of BeO to other oxides. This comparison is done for a constant amount of oxygen. Figure 2.055 shows the Ellingham diagram for BeO and compares BeO to selected oxides. This illustrates that BeO is stable compared to the other oxides, except for Y_2O_3. For example, Be in contact with SiO_2 at 1400 ºC will react to form BeO and Si. However, Y in contact with BeO at 1400 ºC will react to form Y_2O_3 and Be.

3. Mechanical Properties

3.01 Specified Commercial Mechanical Properties

3.011 Materion Corporation:

The mechanical properties of Materion Thermalox 995 BeO ceramic are given in Figure 1.021. The Thermalox 995 BeO is indicated to have the following mechanical properties:

Flexural strength:	30,000 psi (15-25 μm grain size)
	25,000 psi (20-40 μm grain size)
Tensile strength:	18,000 psi
Compressive strength:	225,000 psi
Elastic Modulus:	50×10^6 psi
Poisson's Ratio:	0.26
Hardness:	Rockwell 45N: 60 min.

3.02 Mechanical Properties:

Like all ceramic materials, BeO is brittle at room temperature. This means that it is highly susceptible to fracture if it is mechanically stressed to levels that exceed its fracture strength.

3.021. Single Crystal BeO:

The hexagonal crystal structure of BeO is shown in Figure 3.021. BeO has the wurtzite structure, which can best be described as two identical and interpenetrating hexagonal close-packed lattices. The two arrays are shifted with respect to each other so that points of each lattice lie in the center of the tetrahedral interstices of the other lattice. This shift (z parameter) is equal to 0.375 times the c-axis. The cations occupy the points of one lattice and the anions the other lattice. All the atoms then have tetrahedral coordination, with the tetrahedral of one type all pointing in the same direction along the c-axis. The c/a ratio for BeO is 1.623.

3.0211. Hardness:

The microhardness of BeO single crystals has been investigated (10). Knoop microhardness (100 gm load) was measured on the (0001) basal plane of the BeO crystals. Microhardness values of 1100-1300 kg/mm^2 were reported, with no orientation dependence observed for indentations in the (0001) plane.

3.0212 Strength and Fracture:

The fracture strength of BeO single crystals has been investigated (11). The single crystals were fractured in three-point bending, as shown in Figure 3.0212. Figure 3.0212 shows the bend strength of the BeO single crystals in comparison to the bend strength of polycrystalline BeO material with an 18 μm grain size. The single crystals were considerably stronger than the polycrystalline material. At room temperature, cleavage occurred on both the prismatic and the basal planes.

3.0213. Elastic Constants:

The elastic constants of single crystal BeO have been studied (57-60). Elastic stiffnesses and bulk modulus calculated from the elastic stiffnesses are given in Figure 3.0213.

3.022. Polycrystalline BeO:

3.0221. Elastic moduli:

There have been a limited number of experimental measurements of the elastic moduli of BeO (12-16). Moduli data as a function of grain size are shown in Figure 3.0221-1. The elastic moduli are essentially independent of grain size, as would be expected.

Reference 13 indicates an experimental Young's modulus of 57.5 x 10^6 psi for dense, polycrystalline BeO. This reference also gives calculated values of 42.1 x 10^6 psi for the bulk modulus of BeO and 22.6 x 10^6 psi for the shear modulus. The measured value of Poisson's ratio is given as 0.27. In Reference 14, a Young's modulus value of 56 x 10^6 psi is indicated for fully dense BeO.

Young and shear modulus data for BeO as a function of temperature are shown in Figure 3.0221-2, for both static and dynamic test techniques.

3.0222. Bend strength:

The bend strength of polycrystalline BeO as a function of temperature (4,15,17) is shown in Figure 3.0222. In Figure 3.0222, curve A is for sintered BeO (15), while curve B is for hot pressed BeO (17). These data suggest that the bend strength of hot pressed material may be higher than that of sintered material. However, it should be noted that the sintered BeO was tested in four-point bending (15), while the hot pressed BeO was tested in three-point bending. For a fixed material and bend test specimen size, three-point bending will yield higher bend

strength values than four-point loading, since the volume of material subjected to the highest bending stresses is lower in three-point bending than in four-point bending.

From Figure 3.0222, the room temperature bend strength of sintered BeO is indicated to be 25,000 psi, while the room temperature bend strength of hot pressed BeO is indicated to be 37,000 psi.

3.0223. Tensile strength:

The tensile strength of BeO as a function of temperature is shown in Figure 3.0223. Curve A is from Reference 16. Curve B is from Reference 18. Curve C is from Reference 19. BeO tensile strength generally decreases with increasing temperature.

Curve A is for slip cast material that was 90-94% dense. Curve B is for hot pressed material that was 97.7% dense. Curve C is for hot pressed material that was 98% dense.

At room temperature, the tensile strength of BeO is indicated to be in the range of 12,000-15,000 psi.

3.0224. Compressive strength:

The compressive strength of BeO as a function of temperature is shown in Figure 3.0224. Curve A is from Reference 20. Curve B is from Reference 21. Curve C is from Reference 22. BeO compressive strength generally decreases with increasing temperature. At room temperature, the compressive strength of hot pressed, 98% dense BeO is 300,000 psi.

3.0225. Hardness:

The room temperature Vickers diamond pyramid microhardness of BeO (23) as a function of grain size is shown in Figure 3.0225. The room temperature microhardness increases with increasing BeO grain size, from a value of approximately 800 kg/mm^2 for a grain size of 5 μm to a value of approximately 1000 kg/mm^2 for a grain size of 63 μm. Single crystal BeO microhardness values are also shown (10).

3.0226. Fracture energy and fracture toughness:

The fracture surface energy of BeO has been measured as a function of grain size (24,25). Results are shown in Figure 3.0226. There is the suggestion of a possible increase in fracture energy with increasing grain size, but this does not appear to be a strong trend. The fracture energy of BeO is shown to be higher than that of Al_2O_3. BeO was reported to exhibit considerable transgranular fracture. The fracture toughness of polycrystalline BeO at room temperature is reported to be 4.8 Mpa $m^{1/2}$ (26).

3.0227. Thermal shock:

The thermal shock resistance of polycrystalline BeO has been measured (27,75). Bend specimens were quenched from different temperatures into a water bath and the room temperature strength after quenching from a given temperature was measured. The results (27) are shown in Figure 3.0227. The quenching temperature difference observed to significantly reduce the room temperature strength of BeO was 300 ºC. By comparison, the quenching temperature difference for Al_2O_3 was 200 ºC. This indicates that BeO has a greater thermal shock resistance than Al_2O_3. This is likely due to the higher thermal conductivity of BeO in comparison to Al_2O_3, which will act to reduce thermal stresses.

3.0228. Grain size effects on strength:

The room temperature strength of polycrystalline BeO generally decreases with increasing grain size (12,14,28). Figure 3.0228-1 shows data for sintered BeO (12). Figure 3.0228-2 shows data for hot pressed BeO (28).

3.0229. Environmental effects on strength:

The strength of BeO at room temperature is sensitive to strain rate (28), as shown in Figure 3.0229-1. It increases with increasing strain rate of the mechanical test. Such behavior in ceramic materials is usually attributed to water vapor effects on the brittle fracture process. Figure 3.0229-2 shows the bend strength of BeO as a function of strain rate for tests in both air and water (29). BeO strength increases with increasing strain rate in both air and water.

Figure 3.0229-3 shows crack velocity as a function of stress intensity factor for tests of BeO in a flurocarbon fluid equivalent to that of air at 68% relative humidity (30). This result clearly demonstrates that crack growth in BeO is affected by the humidity of the environment. The data in Figure 3.02293 indicate that the fracture toughness K_{IC} of polycrystalline BeO is 5 MPa $m^{1/2}$.

3.02210. Machining effects on strength:

Machining operations reduce the strength of BeO, as indicated in Figure 3.02210. This is due to the fact that machining operations produce a damaged region on the surface of the BeO, which acts as a source of brittle fracture. When BeO is annealed at 800 ºC after it is machined, its strength recovers to the level before machining, as shown in Figure 3.02210. This is due to the relief of stresses in the machining damaged surface layer of the BeO by the annealing treatment.

3.02211. Creep:

In view of its high melting point, a few studies have been performed on the elevated temperature creep behavior of BeO (31-37). The creep behavior of single crystal BeO (37) is shown in Figure 3.02211-1. The creep rate is highly dependent on crystallographic orientation. BeO is more creep resistant than single crystal Al_2O_3 (sapphire) for both c-axis and a-axis orientations of the applied stress.

Figure 3.02211-2 shows temperature and stress effects on the creep rate of polycrystalline BeO (35). The BeO material studied was 99.5% dense and had a grain size of 63 μm. The activation energy for creep was found to be 145 kcal/mole. The creep rate stress exponent was observed to be 2.5 for creep at 1950 ºC. However, creep exponents of 1 have been observed at lower creep temperatures (32).

A comparison of the creep of BeO in compression and bending (35) is shown in Figure 3.02211-3. The creep rate in bending is indicated to be approximately one order of magnitude higher than the creep rate in compression.

Grain size effects on the creep rate of polycrystalline BeO (34) are shown in Figure 3.02211-4. The creep rate decreases significantly with increasing grain size.

3.02212. Self-Diffusion:

Self-diffusion in BeO has seen limited investigation (38-41). Figure 3.02212 shows the self-diffusion coefficients of Be and O in BeO as a function of temperature (38,39). The values of the diffusion coefficients (in cm^2/sec) as a function of temperature are:

$$D\ (Be) = (2.5 \times 10^{-3})(\exp\ (-62500/RT))$$

$$D\ (O) = (2.95 \times 10^{-5})(\exp\ (-68500/RT))$$

where the activation energy values are in kcal/mole. At a given temperature the diffusion coefficient of oxygen is significantly lower than the diffusion coefficient of beryllium in BeO.

3.02213. Shock Loading:

The dynamic shock loading behavior of BeO has been examined (72-74, 89). The Hugoniot obtained for BeO (72) of initial density 2.84 g/cm^3 is shown in Figure 3.02213-1. The Hugoniot elastic limit was observed to be 82 kbar. The Hugoniot and related data obtained for BeO (73) of initial density 3.0 g/cm^3 is shown in Figure 3.02213-2. The tensile spall strength of dense BeO under dynamic shock loading conditions has been reported to be 80 MPa (74).

The sound velocities reported for fully dense BeO are V_L = 11.99 km s^{-1}, V_S = 7.32 km s^{-1}, and bulk sound velocity C_0 = 8.50 km s^{-1} (89).

4. Fabrication

4.01 Single crystal BeO:

Large single crystals of BeO have been synthesized by a flux growth technique (42-44). Approximately 20 mole % of BeO will dissolve in a Li_2MoO_4-MoO_3 flux (mole ratio 1:1.25) at 1400 ºC, as shown in Figure 4.01-1. However, less than half this amount of BeO is soluble in the flux at its eutectic temperature of approximately 530 ºC. A platinum crucible was used to

contain the flux. BeO crystals approximately 3 mm in size nucleated and grew on the inner surfaces of the crucible during slow cooling. By using seed BeO crystals, larger BeO single crystals could also be grown. A sketch of a BeO single crystal is shown in Figure 4.01-2.

The synthesis of single crystal whiskers of BeO has been reported (76). BeO whiskers 1 μm in diameter and several millimeters in length were produced by heating metallic beryllium filings at 1450-1500 ºC on a BeO support inside a silica glass vessel.

4.02 Polycrystalline BeO:

Polycrystalline BeO components have been fabricated from BeO powders by the processes of sintering and hot pressing.

4.021 BeO powder:

At the present time, the only U.S. source of BeO powder is the Materion Corporation. Figure 4.021 gives specifications on the Materion BeO powder. There are two types of powder, UOX and GC-HF. The UOX powder is smaller in size than the GC-HF powder. UOX powder is typically used for sintering consolidation, while GC-HF powder is typically used for hot pressing consolidation.

There exists an ASTM Standard Specification for Nuclear-Grade Beryllium Oxide Powder, ASTM C 708-72a (reapproved 1977). This ASTM Standard Specification applies to BeO powder used for applications in the nuclear power industry.

4.022 Sintering:

The sintering of polycrystalline BeO has been studied by a number of workers (45-56). Generally, the sintering of BeO without a densification aid requires a higher temperature than the sintering of BeO with a densification aid.

4.0221 Sintering without densification aid:

The sintering behavior of BeO without the use of a densification aid (51) is shown in Figure 4.0221-1. Sintering densification is limited at temperatures below 1500 ºC. The greatest degree of sintering takes place in inert atmospheres and vacuum. Grain growth effects during sintering (48) are shown in Figure 4.0221-2. Significant grain growth with time occurs for sintering temperatures of 1500-1700 ºC.

4.0222 Sintering with densification aid:

The use of lithium oxide (Li_2O) as a densification aid for BeO decreases the temperature required for BeO densification substantially (54). The sintering temperature of BeO is reduced from 1500-1700 ºC to approximately 1000 ºC by the addition of 0.5 wt.% of Li_2O. The enhanced densification resulting from the Li_2O addition is due to the formation of a small

amount of liquid phase resulting from the interaction of Li_2O and BeO to form the compound Li_2BeO_2, which has a melting point less than 950 ºC.

Since the thermal stability of Li_2BeO_2 is poor above its melting point, this compound acts as a fugitive-type flux or densification aid for facilitating liquid phase sintering. Approximately 50% of the Li_2O is lost during the consolidation process and the remainder can be removed by sublimation during a subsequent heat treatment of the sintered body at temperatures in the range of 1000-1500 ºC, without decreasing the density of the BeO.

The lithium oxide employed as the fugitive-type sintering aid may be added as Li_2O or as another lithium compound capable of decomposing to lithium oxide when heated to a temperature less than 950 ºC. Additions of lithium hydroxide (LiOH) and lithium carbonate (Li_2CO_3) have been shown to be effective densification aids for BeO.

4.023 Hot pressing:

The hot pressing of BeO has received a limited amount of study (61-71). All hot pressing studies have employed graphite dies and inert atmospheres. Figure 4.023-1 shows hot pressed density at various temperatures for four different purities of BeO powder (63). No densification aids were employed. Figure 4.023-2 shows the hot pressed microstructure of BeO consolidated from the highest purity powder, powder "D". This material was hot pressed at 1700 ºC and 2000 psi, and was 99.5% dense with a mean grain size less than 20 μm (63).

Densification results of another hot pressing study without densification aids (67) are shown in Figure 4.023-3. In this work, a BeO specimen with a measured density of 3.008 g/cm^3 was produced by hot pressing at 1600 ºC for 25 minutes at 300 kg/cm^2 pressure.

Transparent BeO material has been produced by hot pressing submicron BeO powder at 1200 ºC and 20 kbar pressure (69). It has been reported that when BeO is hot pressed above 1500 ºC, a weak basal plane crystallographic texture develops, with the normals of the basal planes aligned at right angles to the hot pressing direction (62).

The use of lithium-based densification aids such as LiOH and Li_2CO_3 reduces the hot pressing temperature for full densification significantly (71). Figure 4.023-4 shows that the hot pressing temperature for full densification of BeO is reduced to 1000 ºC for densification aid additions of 0.25-1.5 wt.% equivalent of lithium oxide (Li_2O).

4.024 Hot isostatic pressing:

The hot isostatic pressing (HIP) consolidation of BeO has been investigated to a very limited extent (77-82). Submicron BeO powder was enclosed in a platinum capsule and placed in an evacuated and sealed glass tube and hot isostatically pressed at temperatures in the range of 1000-1400 ºC under an isostatic pressure of 2000 kg/cm^2 (77,79). No densification aids were added to the BeO powder. Results are shown in Figure 4.024. Densification to 99.9% theoretical density occurred at a temperature of 1000 ºC without the use of a densification aid.

This result indicates that hot isostatic pressing produces more extensive densification of BeO than hot pressing under similar temperature conditions.

Beryllium-beryllium oxide composites containing 10-70 vol.% BeO have been produced by HIPing at temperatures from 900 ºC to 1277 ºC (the melting point of beryllium) (82).

4.025. Machining and Grinding:

There are relatively few references on the machining of BeO (83-87). Since BeO is a hard ceramic and an electrical insulator, its machining requires diamond tooling. In surface grinding operations, resin bonded diamond wheels which generally contain 100/120 US mesh grit at 100 concentration have been used (85).

Annealing of machined surfaces of BeO has been shown to lead to increases in strength (86), as shown in Figure 4.025-1. Effects of grain size on the strength of machined BeO and machined/annealed BeO are shown in Figure 4.025-2.

Microwave annealing of machined BeO at 950 ºC using 24 GHz microwaves to heat the BeO directly has been reported to heal surface and near surface microcracks and as a result increase the room temperature strength of BeO (88). The four-point bend strength of BeO fabricated by hot pressing was observed to increase from 23,790 psi for as-machined surfaces, to 32,070 for microwave annealed surfaces. A liquid phase was observed on the surfaces of the microwave annealed BeO material.

References:

1. M.T. Pavlova, P. Wambach, D.W. Harvey, "Communicating Health Risks Working Safely With Beryllium", Oak Ridge National Laboratory Report, May 1998.

2. Z. Wang, P.S. White, M. Petrovic, O.L. Tatum, L.S. Newman, L.A. Maier, B.L. Marrone, "Differential Susceptibilities to Chronic Beryllium Disease Contributed by Different Glu^{69} HLA-DPB1 and –DPA1 Alleles", Journal of Immunology, 163, 1647-1653 (1999).

3. Department of Energy Final Rule 10 CRF 850, "Chronic Beryllium Disease Prevention Program (CBDPP)", 8 December 1999.

4. "Engineering Property Data on Selected Ceramics, Volume III, Single Oxides", Metals and Ceramics Information Center Report MCIC-HB-07-Vol. III, Battelle Columbus Laboratories, Columbus, Ohio, July 1981.

5. W.D. Kingery, H.K. Bowen, D.R. Uhlmann, "Introduction to Ceramics", second edition, John Wiley & Sons, New York, c. 1976.

6. J.D. Fowler Jr., "Radio Frequency Heating of Ceramic Windows in Fusion Applications", Los Alamos National Laboratory Report LA-9088-MS, November 1981.

7. P.J. Spencer, O. von Goldbeck, R. Ferro, K. Girgis, A.L. Dragoo, "Beryllium: Physico-Chemical Properties of its Compounds and Alloys", editor: O. Kubaschewski, Special Issue No. 4, International Atomic Energy Agency, Vienna, 1973.

8. W.I. Stuart and G.H. Price, "The High Temperature Reaction Between Beryllia and Water Vapour", Journal of Nuclear Materials, 14, 417-424 (1964).

9. J.R. Stehn, "The Nuclear Properties of Beryllium", pp. 328-366 in "The Metal Beryllium", Eds. D.W. White Jr. and J.E. Burke, The American Society for Metals, Cleveland, Ohio, c. 1955.

10. C.F. Cline and J.S. Kahn, "Microhardness of Single Crystals of BeO and Other Wurtzite Compounds", Journal of the Electrochemical Society, 110, 773-775 (1963).

11. G.C. Bentle and K.T. Miller, "Dislocations, Slip, and Fracture of BeO Single Crystals", Journal of Applied Physics, 38, 4248-4257 (1967).

12. R.E. Fryxell and B.A. Chandler, "Creep, Strength, Expansion, and Elastic Moduli of Sintered BeO as a Function of Grain Size, Porosity, and Grain Orientation", Journal of the American Ceramic Society, 47, 283-291 (1964).

13. J.S. O'Neill, "Strength and Elastic Modulus Relationships in BeO-SiC Bodies", Trans. British Ceramic Society, 69, 81-84 (1970).

14. J.S. O'Neill, N.A. Hill, and D.T. Livey, "Observations on the Strength and Young's Modulus of BeO as a Function of Density and Grain Size", Proceedings, British Ceramic Society, 6, 95-101 (1966).

15. R.E. Fryxell and B.A. Chandler, "Creep, Strength, Expansion, and Elastic Moduli of Sintered BeO as a Function of Grain Size, Porosity, and Grain Orientation", Journal of the American Ceramic Society, 47, 283-291 (1964).

16. B. Schwartz, "Beryllia, Its Physical Properties at Elevated Temperatures", Massacusetts Institute of Technology Report 1083, ATI-210826 (27 February 1952).

17. S.C. Carniglia, R.E. Johnson, A.C. Hott, and G.G. Bentle, "Hot Pressing for Nuclear Application of BeO: Process, Product, and Properties", Journal of Nuclear Materials, 14, 378-394 (1964).

18. J.J. Gangler, "Some Physical Properties of Eight Refractory Oxides and Carbides", Journal of the American Ceramic Society, 33, 367-374 (1950).

19. R.C. Emanuelson, "Electrical, Mechanical, and Thermal Properties of Hot Pressed and Sintered Beryllium Oxide", Paper APR-1048 presented at the 15th Pacific Coast Regional Meeting of the American Ceramic Society, Seattle, Washington, 17-19 October 1962.

20. R.C. Emanuelson, "Electrical, Mechanical and Thermal Properties of Hot-Pressed and Sintered BeO", Supplement No. 1, APR-1048 (June 12, 1963).

21. E. Ryshkewitch, "The Compressive Strength of Pure Refractories", Berichte der Deutschen Keramischen Gesellschaft, 22, 54-65 (February 1941).

22. I. Ya. Guzman and D.C. Poluboyarinov, "Some Properties of Porous Ceramics May of Beryllium Oxide", Ogneupory, 10, 10-19 (1962).

23. R.W. Armstrong, E.L. Raymond, and R.R. Vandervoort, "Anomalous Increase in Hardness with Increase in Grain Size of Beryllia", Journal of the American Ceramic Society, 53, 529-530 (1970).

24. P.L. Gutshall and G.E. Gross, "Fracture Energy of Polycrystalline Beryllium Oxide", Journal of the American Ceramic Society, 51, 602 (1968).

25. J.F. Lynch and R.C. Bradt, "Work of Fracture of BeO", Journal of the American Ceramic Society, 56, 228-229 (1973).

26. P.F. Becher and M.K. Ferber, "Mechanical Reliability of Ceramic Windows in High Frequency Microwave Heating Devices", Journal of Materials Science, 19, 3778-3785 (1984).

27. D.A. Krohn, D.R. Larson, and D.P.H. Hasselman, "Comparison of Thermal-Stress Resistance of Polycrystalline Al_2O_3 and BeO", Journal of the American Ceramic Society, 56, 490-491 (1973).

28. G.G. Bentle and R.M. Kniefel, "Brittle and Plastic Behavior of Hot-Pressed BeO", Journal of the American Ceramic Society, 48, 570-577 (1965).

29. W.B. Rotsey, K. Veevers, and N.R. McDonald, "The Effect of Strain Rate, Environment, and Surface Condition on the Modulus of Rupture of Beryllia", Proceedings, British Ceramic Society, 7, 205-219 (1967).

30. M.K. Ferber and Paul F. Becher, "Static Fatigue Behavior of Polycrystalline Beryllia", Journal of the American Ceramic Society, 73, 2038-2046 (1990).

31. R. Chang, "High Temperature Creep and Anelastic Phenomena in Polycrystalline Refractory Oxides", Journal of Nuclear Materials, 2, 174-181 (1959).

32. R.R. Vandervoort and W.L. Barmore, "Compressive Creep of Polycrystalline Beryllium Oxide", Journal of the American Ceramic Society, 46, 180-184 (1963).

33. S.B. Austerman and R. Chang, "Diffusion and Creep in Beryllium Oxide", Journal of Nuclear Materials, 12, 337-339 (1964).

34. W.L. Barmore and R.R. Vandervoort, "High-Temperature Plastic Deformation of Polycrystalline Beryllium Oxide", Journal of the American Ceramic Society, 48, 499-505 (1965).

35. W.L. Barmore and R.R. Vandervoort, "High-Temperature Creep and Dislocation Etch Pits in Polycrystalline Beryllium Oxide", Journal of the American Ceramic Society, 50, 316-320 (1967).

36. M.S. Seltzer, "Correlation Between Activation Energies for Steady-State Creep and Self-Diffusion in Beryllium Oxide", Journal of Nuclear Materials, 26, 232-234 (1968).

37. G.S. Corman, "Creep of Beryllia Single Crystals", Journal of the American Ceramic Society, 75, 71-76 (1992).

38. H.J. De Bruin and G.M. Watson, "Self-Diffusion of Beryllium in Unirradiated Beryllium Oxide", Journal of Nuclear Materials, 14, 239-247 (1964).

39. J.B. Holt, "Self-Diffusion of Oxygen in Single-Crystal Beryllium Oxide", Journal of Nuclear Materials", 11, 107-110 (1964).

40. S.B. Austerman, "Self-Diffusion in Beryllium Oxide", Journal of Nuclear Materials, 14, 248-257 (1964).

41. S.B. Austerman and R. Chang, "Diffusion and Creep in Beryllium Oxide", Journal of Nuclear Materials, 12, 337-339 (1964).

42. S.B. Austerman, "Growth of Beryllia Single Crystals", Journal of the American Ceramic Society, 46, 6-10 (1963).

43. S.B. Austerman, "Growth and Properties of Beryllium Oxide Single Crystals", Journal of Nuclear Materials, 14, 225-236 (1964).

44. S.B. Austerman, "Flux Process for Growth of Large Crystals with Application to Beryllia", Journal of Crystal Growth, 42, 284-288 (1977).

45. B.R. Steele, N.S. Hibbert, F. Rigby, B. Oldfield, and F.S. Martin, "The Preparation and Characterization of Ceramic Grade BeO", Journal of Nuclear Materials, 14, 310-314 (1964).

46. M.J. Bannister, "Sinterability Studies on Various BeO Powders", Journal of Nuclear Materials, 14, 303-309 (1964).

47. D.T. Livey and A.W. Hey, "Sintering and Densification Studies on BeO Powders", Journal of Nuclear Materials, 14, 285-293 (1964).

48. M.J. Bannister, "The Kinetics of Sintering and Grain Growth of Beryllia", Journal of Nuclear Materials, 14, 315-321 (1964).

49. R.J. Brown and N.W. Bass, "Fabrication and Properties of Commercial Beryllia Ceramics for Nuclear Applications", Journal of Nuclear Materials, 14, 341-348 (1964).

50. T.E. Clare, "Studies in the Cold Pressing and Sintering of Beryllia", Journal of Nuclear Materials, 14, 359-367 (1964).

51. W.W. Beaver, J.G. Theodore, and C.A. Bielawski, "Effects of Powder Characteristics, Additives and Atmosphere on the Sintering of Sulfate-Derived BeO", Journal of Nuclear Materials, 14, 326-337 (1964).

52. J. Bardsley and A. Ridal, "The Development of a Technique for Extrusion and Sintering of Beryllia", Journal of Nuclear Materials, 14, 368-377 (1964).

53. T. Ikegami, S. Matsuda, Y. Moriyoshi, and H. Suzuki, "Sintering Processes of a Sinterable and a Nonsinterable BeO Powder", Journal of the American Ceramic Society, 61, 532-533 (1978).

54. U.S. Patent No. 3,529,046, "Utilizing Lithium Oxide and Precursors as Sintering Aid for Hot Pressing Beryllium Oxide", Rudolph Hendricks Jr., 15 September 1970.

55. R. Bhat, V.K. Moorthy, A. Mohan, and N.C. Soni, "Kinetic Studies on Sintering of BeO", Trans. Indian Ceramic Society, 39, 120-126 (1980).

56. A.V. Khudyakov, "Reasons for Accelerated Sintering of Beryllium Oxide Powder Containing Helium", Inorganic Materials, 21, 688-692 (1985).

57. G.G. Bentle, Journal of the American Ceramic Society, 49, 125 (1966).

58. C.F. Cline, H.L. Dunegan, and G.W. Henderson, Journal of Applied Physics, 38, 1944 (1967).

59. N.N. Sirota, A.M. Kuzmina, and N.S. Orlova, Dokl. Akad. Nauk SSSR, 314, 856 (1990).

60. V. Milman and M.C. Warren, "Elasticity of Hexagonal BeO", Journal of Physics: Condensed Matter, 13, 241-251 (2001).

61. C.S. Smith, "Beryllium Oxide", Chapter 3 of Volume 10 "Metallurgy", Los Alamos Scientific Laboratory Report LA-1236 (1945).

62. J.W. Kelly, "The Texture of Hot-Pressed Beryllium Oxide", Journal of Nuclear Materials, 8, 227-231 (1963).

63. S.C. Carniglia, R.E. Johnson, A.C. Hott, and G.G. Bentle, "Hot Pressing for Nuclear Applications of BeO: Process, Product, and Properties", Journal of Nuclear Materials, 14, 378-394 (1964).

64. R.E. Johnson, "Hot-Pressing High-Density Small Grain Size Beryllia", American Ceramic Society Bulletin, 43, 886-888 (1964).

65. K. Langrod, "Graphite as Grain Growth Inhibitor in Hot-Pressed Beryllium Oxide", Journal of the American Ceramic Society, 48, 110-111 (1965).

66. I. Amato, R.I. Colomb, and M. Ravizza, "Hot-Pressing of Beryllia and Zirconia", Journal of Nuclear Materials, 22, 97-99 (1967).

67. J. Bardsley and G. Wulf, "Hot Pressing of Beryllium Oxide with Additives", Australian Atomic Energy Commission Research Establishment Report AAEC-TM-440 (1968).

68. P.P. Budnikov, V.I. Kushakovskii, and B.A. Zhidkov, "Hot Pressing of Beryllium Oxide and Strength of the Pressed Specimens", J. Appl. Chem. USSR, 43, 2107-2109 (1970).

69. K. Kodaira and M. Koizumi, "Fabrication of Transparent BeO by High-Pressure Hot-Pressing", Materials Research Bulletin, 6, 261-265 (1971).

70. J.A. Rubin and W.J. Gardner, "Hot Pressed Beryllia. Final Technical Report, June 1972-January 1973", Report No. AD-787847, Ceradyne Inc., Chatsworth, California, 29 October 1973.

71. U.S. Patent No. 4,762,656, "Method for Hot Pressing Beryllium Oxide Articles", Ambrose H. Ballard, Thomas G. Godfrey Jr., E.H. Mowery, 9 August 1988.

72. W.H. Gust and E.B. Royce, "Dynamic Yield Strengths of B_4C, BeO, and Al_2O_3 Ceramics", Journal of Applied Physics, 42, 276-295 (1971).

73. S.P. Marsh, "LASL Shock Hugoniot Data", University of California Press, Berkeley, c. 1980.

74. D. Yaziv, S.J. Bless, and D.P. Dandekar, "Shock Compression and Spall in Porous Beryllium Oxide", Conference on Metallurgical Applications of Shock-Wave and High-Strain-Rate Phenomena, Marcel Dekker Inc. (Mechanical Engineering 52), New York, c. 1986.

75. R.W. Swindeman, "Thermal Shock Tests on Beryllia", Journal of Nuclear Materials, 14, 404-415 (1964).

76. P.P. Budnikov and D.B. Sandulov, "Preparation and Investigation of Filamentary Single Crystals (Whiskers) of Beryllium Oxide", Zhurnal Prikladnoi Khimii, 43, 1649-1653 (1970).

77. K. Kodaira, M. Shimada, S. Kume, and M. Koizumi, "Hot Isostatic Pressing of Glass-Sealed BeO", Materials Research Society Bulletin, 7, 551-556 (1972).

78. M. Koizumi, K. Kodaira, M. Shimada, S. Saito, H.D. Batha, J.A. Pask, Y. Kotera, and S. Somiya, "Hot Isostatic Pressing of BeO", in "Equilibria and Kinetics in Modern Ceramic Processing", U.S.-Japan Seminar on Basic Science of Ceramics (28 April 1972, Berkeley, California), Publisher: Tokyo Insititute of Technology, c. 1972.

79. K. Kodaira, T. Matsushita, M. Koizumi, M. Shimada, and S. Kume, "Hot Isostatic Pressing of Beryllium Oxide", Yogyo-Kyokai-Shi, 81, 520-523 (1973).

80. R. Hendrick, A.H. Ballard, W.E. Steinkam, and T.E. Walters, "Isostatic Hot-Pressing of Beryllium Oxide", American Ceramic Society Bulletin, 53, 319 (1974).

81. K. Kodaira, T. Matsushita, and M. Koizumi, "Sintering of BeO Under Hydrostatic Pressure of 20 Kbars", Memoirs of the Faculty of Engineering, Hokkaido University, 14, 107-111 (1975).

82. U.S. Patent No. 5,124,119, "Method of Making Beryllium-Beryllium Oxide Composites", Fritz C. Grensing, 23 June 1992.

83. K. Veevers and W.B. Rotsey, "The Effect of Machining on the Modulus of Rupture of Extruded and Sintered BeO", Journal of Nuclear Materials, 15, 133-134 (1965).

84. W.J. Wright, "Machining of Nuclear Materials", Prod. Eng., 46, 638-650 (1967).

85. "Machining an Unusual Ceramic", Ind. Diamond Rev., 29, 116-117 (1969).

86. K. Veevers, "Recrystallisation of Machined Surfaces of Beryllium Oxide", J. Aust. Ceram. Soc., 5, 16-20 (1969).

87. A.W. Hey and G. Martin, "Fabrication, Properties, and Applications of Beryllium and Beryllium Oxide in Electrical Engineering. Part 1", Elektro-Anz., 24, 147-148 (1971).

88. M.S. Morrow, D.E. Schechter, R. Simandl, H.E. Huey, and Q.S. Wang, "A Comparison of Annealing Treatments of an Oxide Ceramic", Ceramic Engineering and Science Proceedings, 20, 207-212 (1999).

89. S.P. Marsh, "Hugoniot Equation of State of Beryllium Oxide", High Temperatures-High Pressures, 5, 503-508 (1973).

90. Outokumpu HSC Chemistry for Windows, Version 4.0, Chemical Reaction and Equilibrium Software with Extensive Thermochemical Database, June 1999.

91. L.P. Belykh and A.N. Nesmeyanov, "Measurements of the Vapor Pressure of Solid Beryllium Oxide", Proceedings of the Academy of Sciences of the USSR, Physical Chemistry Section, 128, 827-828 (1959).

92. V.V. Kandyba, P.B. Kantor, R.M. Krasovitsskaya, and E.N. Fomichev, "Determination of Enthalpy and Thermal Capacity of Beryllium Oxide in the Temperature Range from 1200-2820 K", Doklady Akad. Nauk SSSR, 131, 566-567 (1960).

93. A.C. Victor and T.B. Douglas, "Thermodynamic Properties of Magnesium Oxide and Beryllium Oxide from 298 to 1200 K", J. Res. Natl. Bur. Std., 67A, 325-329 (1963).

94. F.J. Krieger, "The Thermodynamics of the Beryllia/Beryllium-Oxygen Vapor System", RAND Corporation Report RM-5151-PR (1966).

95. E.E. Shpiel'rain, D.N. Kagan, and L.S. Barkhatov, "Thermodynamic Properties of Beryllium Oxide in the Liquid and Solid Phases", High Temp. (USSR) (Engl. Transl.), 9, 842-844 (1971).

96. E.E. Shpiel'rain, D.N. Kagan, and L.S. Barkhatov, "Study of Thermodynamical Properties of Beryllium Oxide in Phase Transition Area", Revue Internationale des Hautes Temperatures et des Refractaires, 12, 19-22 (1975).

BeO BRUSHWELLMAN
ENGINEERED MATERIALS

SALES/ORDERS: 6100 Tucson Blvd. • Tucson, AZ 85706 • 800-626-5351 • 602-746-0251 • FAX: 602-294-8906
TECHNICAL INFORMATION: 17876 St. Clair Ave. • Cleveland, OH 44110 • 800-321-2076 • 216-486-4200 • FAX: 216-383-4091

SPECIFICATION SHEETS

ISOPRESSED THERMALOX 995 CERAMICS

CDI-20, Rev. B

Orig. Issue	Sept 24, 1971
Rev. A	June 15, 1974
Rev. B	July 11, 1984

1. GENERAL PROVISIONS

1.1 Brush Wellman Inc. will provide written Certification of Compliance to this specification or to an approved customer specification upon request.

1.2 Normal inspection is performed in accordance with MIL-STD-105D, General Level II, 2.5 AQL (non-cumulative) or equivalent.

1.3 The term "Lot" is defined to include parts formed from the same powder batch and fired in the same kiln firing.

1.4 Visual defects are defined according to ASTM F-109-79.

1.5 All dimensions are interpreted per USASI-Y14.5-66.

1.6 The products produced to this specification are required to meet all criteria which apply except Typical Properties, Section 4. Properties listed in this section must be specified individually by the customer in order for outgoing products to be specifically tested and accepted to these requirements.

2. CHEMICAL COMPOSITION

2.1 Chemical composition as used in this specification is defined as % purity = 100%-% by weight of total metallic impurity. The metallic impurity content is determined by emission spectroscopy.

3. TEST CONDITION

3.1 All physical, mechanical and electrical tests are performed at room temperature, except where noted.

Figure 1.021: Commercial specifications for Materion Isopressed Thermalox 995 BeO.

4.0 TYPICAL PROPERTIES

Property	Test Method	Value
4.1 Chemical 4.1.1 BeO Content	Spectrographic Analysis (100%-% by wt. of total metallic impurities)	99.5% min.
4.2 Thermal 4.2.1 Coefficient of Thermal Expan.	ASTM E-228-71	(25-1000°C) 9.0 X 10^{-6}/° C
4.2.2 Conductivity	Axial Rod Method	@ 25° C 0.60 cal/(cm. sec.° C) min. @ 100° C 0.45 cal/(cm. sec.° C) min. @ 150° C 0.35 cal/(cm. sec.° C) min.
4.2.3 Specific Heat	ASTM C-351-73	0.25 cal/(gm.° C)
4.3 Electrical 4.3.1 Dielectric Constant	ASTM D-150-74 ASTM D-2520-70	@ 1 MHz 6.5 @ 10 GHz 6.6
4.3.2 Dissipation Factor	ASTM D-150-74 ASTM D-2520-70	@ 1 MHz 0.0004 max. @ 10 GHz 0.0004 max.
4.3.3 Resistivity	ASTM D-257-76	$>10^{15}$ ohm-cm
4.3.4 Dielectric Strength	ASTM D-149-75	1/4" thick 240 V/mil
4.4 Physical 4.4.1 Density	ASTM C-373-72	2.85 g/cm^3, min. avg.
4.4.2 Impenetrability, Gas	He-Mass Spec.	10^{-8} cc/sec. Helium
4.4.3 Impenetrability, Liquid	ASTM D-116-76 or other dye penetrants	Impervious
4.4.4 Hardness	ASTM E-18-74	Rockwell 45N 60 min.
4.4.5 Grain Size	Linear intercept	Standard Parts 15-25 μm Massive Parts 20-40 μm
4.5 Mechanical 4.5.1 Flexural Strength	ASTM F-417-75	15-25 μm Grain Size 30,000 psi 20-40 μm Grain Size 25,000 psi
4.5.2 Modulus of Elasticity	ASTM C-623-75	50 X 10^6 psi
4.5.3 Poisson's Ratio	ASTM C-565-71	0.26
4.5.4 Tensile Strength	ASTM C-565-71	18,000 psi
4.5.5 Compressive	ASTM C-773-4	225,000 psi

4.6 LARGE PARTS

Parts which require especially long firing cycles due to their size have coarser grains and lower mechanical strengths. Such parts typically include machining stock or parts whose minimum dimension exceeds one inch.

There may be variation of properties within large parts. The outgoing quality of the large parts is required to conform to the bulk or sampled properties set forth below. Variation within the large parts not detected in the above tests is considered normal to this product and is not cause for return or rejection.

On the basis of bulk testing or limited sampling of material near the surface the large parts shall meet the following properties:
4.6.1 Bulk density 2.85 minimum.
4.6.2 Grain size 15 - 40μm.
4.6.3 Flexural strength 25,000 psi minimum average.

Figure 1.021: Commercial specifications for Materion Isopressed Thermalox 995 BeO.

5.0 AS-FIRED DIMENSIONAL TOLERANCES

Dimensional Tolerances (in inches)	Class 1	Class 2	Class 3
5.1 Tubes 5.1.1 Outside diameter	±2%, NLT 1/32	±2%, NLT 1/16	±6%, NLT 1/8
5.1.2 Inside diameter	±1%, NLT 0.003	±1½%, NLT 0.005	±2%, NLT 0.010
5.1.3 Length	±2%, NLT 1/32	±4%, NLT 1/16	±6%, NLT 1/8
5.1.4 Concentricity	±2%, NLT 0.005	±5%, NLT 0.010	±10%, 0.025
5.1.5 Camber, max.	0.001 in/in	0.003 in/in	0.006 in/in
5.1.6 Ellipticity (roundness)	Within dimensional tolerances		
5.2 Rods 5.2.1 Outside diameter	±2%, NLT 1/32	±4%, NLT 1/16	±6%, NLT 1/8
5.2.2 Length	±2%, NLT 1/32	±4%, NLT 1/16	±6%, NLT 1/8
5.2.3 Camber, max.	0.001 in/in	0.003 in/in	0.006 in/in
5.3 Bars, Plate, Blocks 5.3.1 Width & thickness	±2%, NLT 1/32	±4%, NLT 1/16	±6%, NLT 1/8
5.3.2 Length	±2%, NLT 1/32	±4%, NLT 1/16	±6%, NLT 1/8
5.3.3 Flat & Parallel	Within dimensional tolerances		

Notes: 1. Bars, plates & blocks have 1/8" nominal radius.

2. For extreme thin sections, some exceptions may be required.

6.0 VISUAL DEFECT CRITERIA

	Machined	Machined	As Fired Blank
Visual Defects ASTM F-109 Definitions (units in inches)	Level 1 Max.	Level 2 Max.	Level 3 Max.
6.1 Blemish	None	0.030	0.100
6.2 Blister	None	0.015	0.030
6.3 Burr, Fin Flash	None	None	Within dimensional tolerance
6.4 Chip (open or closed-length unlimited) 6.4.1 Parts up to 0.5 L or dia.	0.015W X 0.015 D	0.020 W X 0.020 D	Width & depth within dimensional tolerance
6.4.2 Parts 0.5 to 1.0 L or dia.	0.020-W X 0.020 D	0.030 W X 0.030 D	Width & depth within dimensional tolerance

Figure 1.021: Commercial specifications for Materion Isopressed Thermalox 995 BeO.

VISUAL DEFECT CRITERIA (continued from previous page)

	Machined	Machined	As Fired Blank
6.4.3 Parts 1.0 to 2.0 L or dia.	0.025 W x 0.025 D	0.040 W x 0.040 D	Width & depth within dimensional tolerance
6.4.4 Parts over 2.0 L or dia.	0.030 W x 0.030 D	0.050 W x 0.050 D	Width and depth within dimensional tolerance
6.5 Cracks & Laminations	None	Less than 0.015 from edge into part	Within dimensional tolerance
6.6 Grinding Marks	Within surface finish tolerance See 7.13	Within surface finish tolerance See 7.13	—
6.7 Inclusion	None	0.010	0.030
6.8 Pit, Pock, Hole, Porous Area, (surface dimension)	0.015	0.025	0.050

7.0 MACHINED DIMENSIONAL TOLERANCES

Dimensional Tolerances, Inches	Class 1	Class 2	Class 3	Class 4
7.1 Length (outside)	±0.0005	±0.001	±0.005	±0.010
7.2 Diameter (O.D.)	±0.0005	±0.001	±0.005	±0.010
7.3 I.D., tubes	±0.0005	±0.001	±0.005	±0.010
7.4 Hole Diameter	±0.0005	±0.001	±0.005	±0.010
7.5 Hole location	±0.001	±0.005	±0.010	—
7.6 Concentricity, TIR	0.001	0.005	0.010	—
7.7 Ellipticity (roundness)	Within dimensional tolerances			
7.8 Radius	±0.001	±0.005	±0.010	—
7.9 Angle, degree	± ½	±1	±2	±5
7.10 Flatness (plates) TIR	0.0005	0.001	0.002	0.005
7.11 Camber (rods & tubes) in/in, max.	0.0005	0.001	0.0015	0.002
7.12 Parallelism, TIR	0.0005	0.001	0.002	0.005
7.13 Surface Finish RMS, Microinches, max.	32	64	64	—

Figure 1.021: Commercial specifications for Materion Isopressed Thermalox 995 BeO.

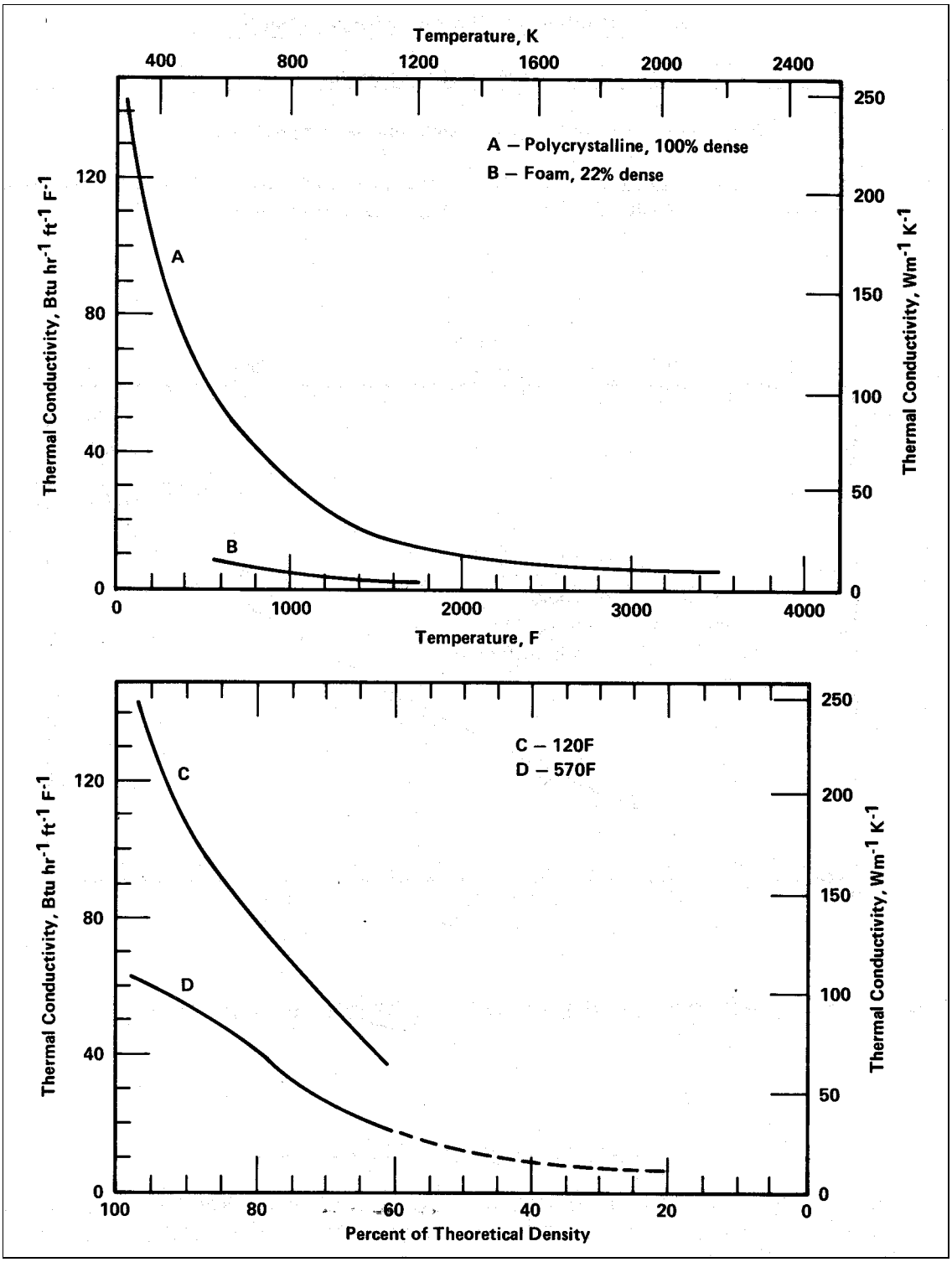

Figure 2.013: Thermal conductivity of polycrystalline BeO as a function of temperature and density (4).

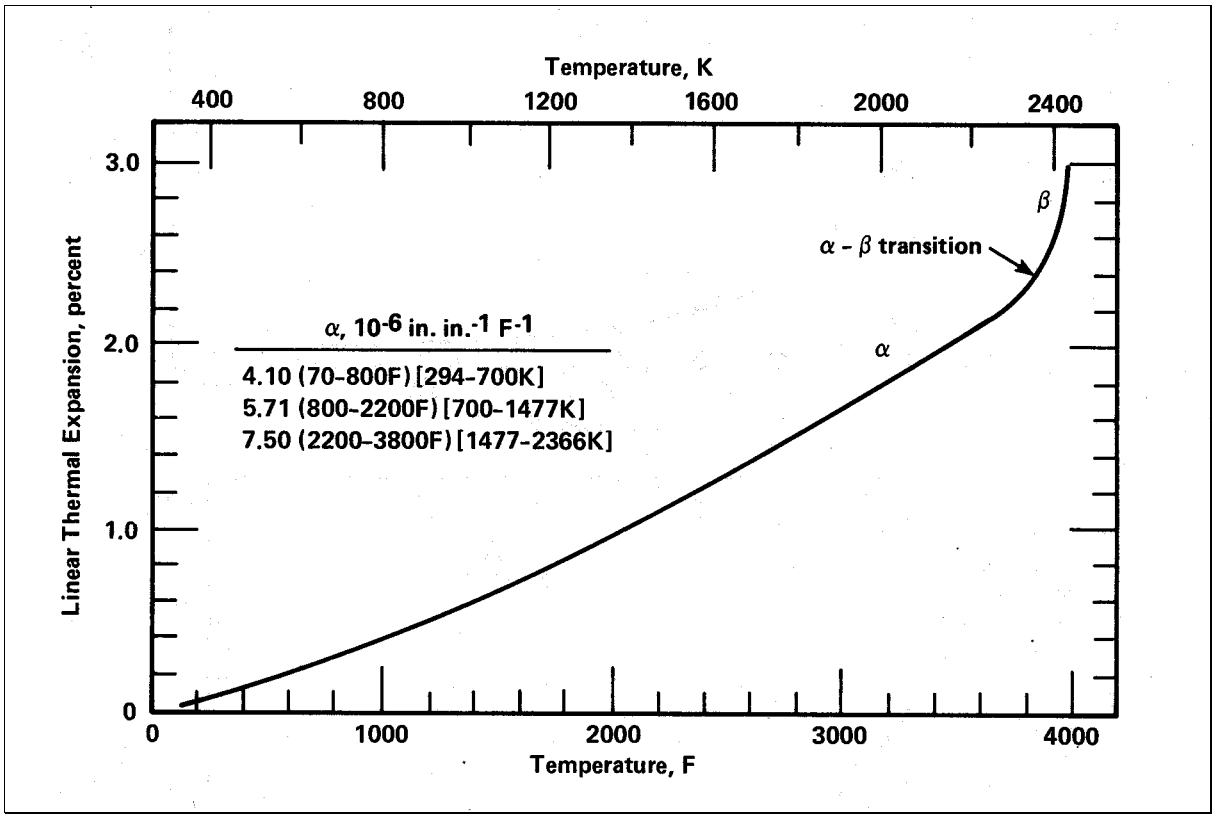

Figure 2.014: Thermal expansion of BeO as a function of temperature (4).

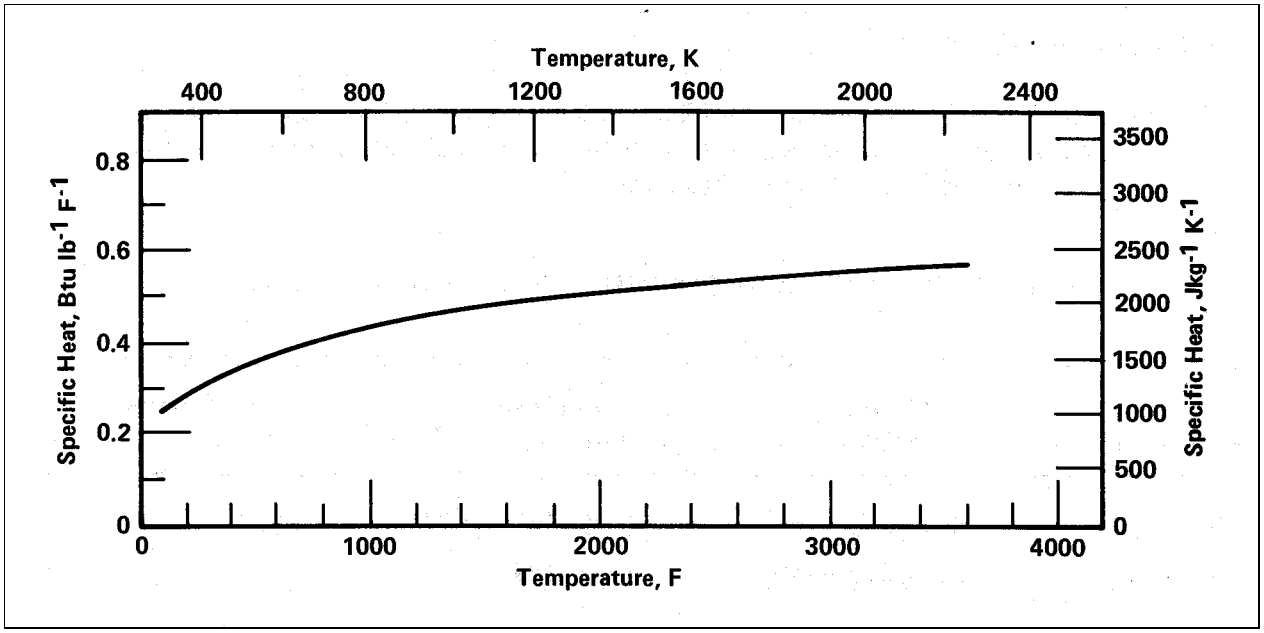

Figure 2.015: Specific heat of BeO as a function of temperature (4).

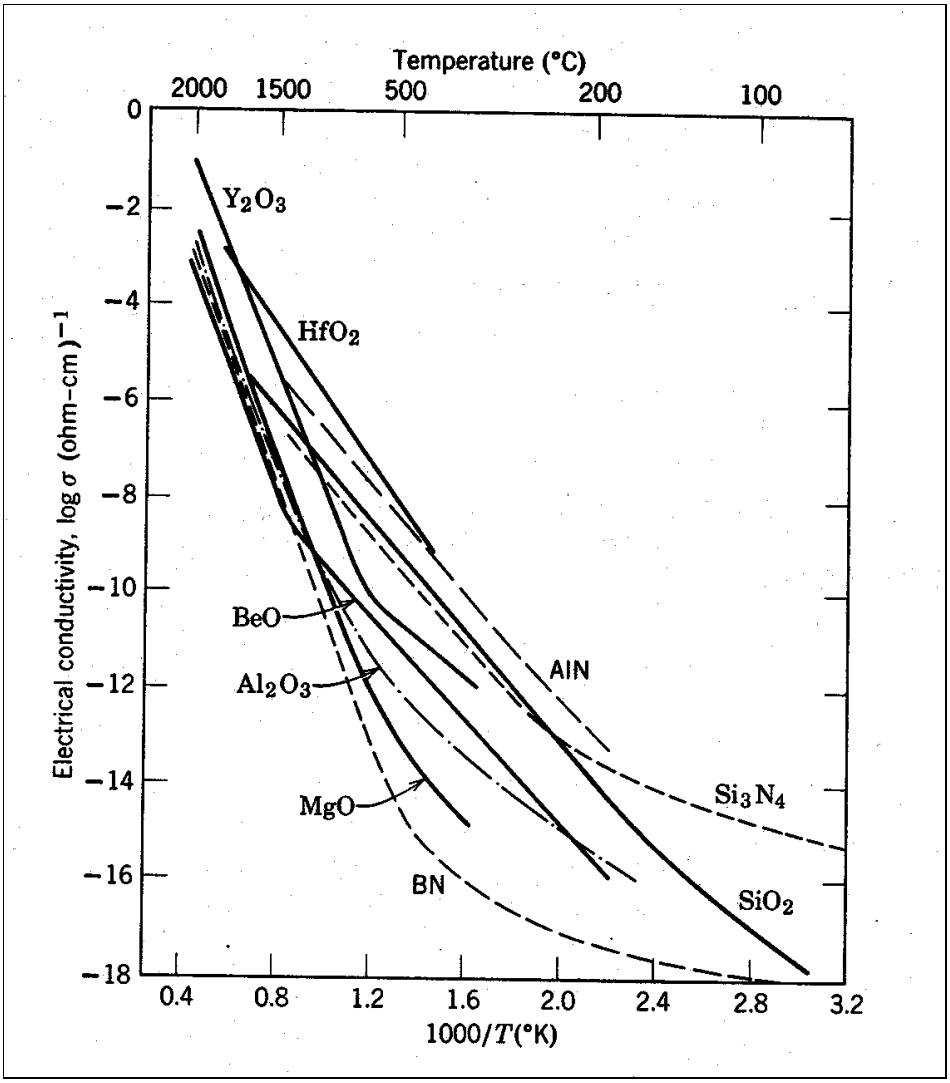

Figure 2.0221: Electrical conductivity of BeO as a function of temperature (5).

Rates of Vaporization and Vapor Pressures of Beryllium Oxide

Temperature, °K	Area of orifice, cm^2	Duration of experiment, sec	Weight of condensate, g	Rate of vaporization, $g/cm^2 \cdot sec$	Pressure, atmos
2573	$1,37 \cdot 10^{-3}$	2640	$2,42 \cdot 10^{-4}$	$7,181 \cdot 10^{-5}$	$1,53 \cdot 10^{-5}$
2508	$1,03 \cdot 10^{-3}$	3600	$1,30 \cdot 10^{-4}$	$3,507 \cdot 10^{-5}$	$7,94 \cdot 10^{-6}$
2463	$1,03 \cdot 10^{-3}$	1200	$2,25 \cdot 10^{-4}$	$1,820 \cdot 10^{-5}$	$4,07 \cdot 10^{-6}$
2453	$2,74 \cdot 10^{-3}$	3900	$1,39 \cdot 10^{-4}$	$1,301 \cdot 10^{-5}$	$2,91 \cdot 10^{-6}$
2378	$1,03 \cdot 10^{-3}$	3900	$3,24 \cdot 10^{-5}$	$8,066 \cdot 10^{-6}$	$1,78 \cdot 10^{-6}$
2373	$2,74 \cdot 10^{-3}$	1800	$3,33 \cdot 10^{-5}$	$6,752 \cdot 10^{-6}$	$1,49 \cdot 10^{-6}$
2333	$2,74 \cdot 10^{-3}$	2700	$4,44 \cdot 10^{-5}$	$6,002 \cdot 10^{-6}$	$1,31 \cdot 10^{-6}$
2308	$1,13 \cdot 10^{-1}$	1500	$5,82 \cdot 10^{-4}$	$3,434 \cdot 10^{-6}$	$7,45 \cdot 10^{-7}$
2293	$2,74 \cdot 10^{-3}$	2760	$2,38 \cdot 10^{-5}$	$3,147 \cdot 10^{-6}$	$6,80 \cdot 10^{-7}$
2263	$2,74 \cdot 10^{-3}$	2700	$4,16 \cdot 10^{-6}$	$5,623 \cdot 10^{-7}$	$1,21 \cdot 10^{-7}$
2203	$1,13 \cdot 10^{-1}$	3600	$2,77 \cdot 10^{-4}$	$6,814 \cdot 10^{-7}$	$1,45 \cdot 10^{-7}$
2213	$2,74 \cdot 10^{-3}$	4200	$6,10 \cdot 10^{-6}$	$5,301 \cdot 10^{-7}$	$1,13 \cdot 10^{-7}$
2183	$1,13 \cdot 10^{-1}$	4200	$1,94 \cdot 10^{-4}$	$4,088 \cdot 10^{-7}$	$8,61 \cdot 10^{-8}$
2163	$2,74 \cdot 10^{-3}$	18300	$1,66 \cdot 10^{-5}$	$3,311 \cdot 10^{-7}$	$6,95 \cdot 10^{-8}$
2153	$1,13 \cdot 10^{-1}$	1200	$3,33 \cdot 10^{-5}$	$2,456 \cdot 10^{-7}$	$5,14 \cdot 10^{-8}$
2128	$1,13 \cdot 10^{-1}$	1500	$3,17 \cdot 10^{-5}$	$1,870 \cdot 10^{-7}$	$3,89 \cdot 10^{-8}$
2103	$1,13 \cdot 10^{-1}$	3600	$3,33 \cdot 10^{-5}$	$8,186 \cdot 10^{-8}$	$1,70 \cdot 10^{-8}$

Figure 2.031: Measured vapor pressure of BeO from 2100-2570 °K (91).

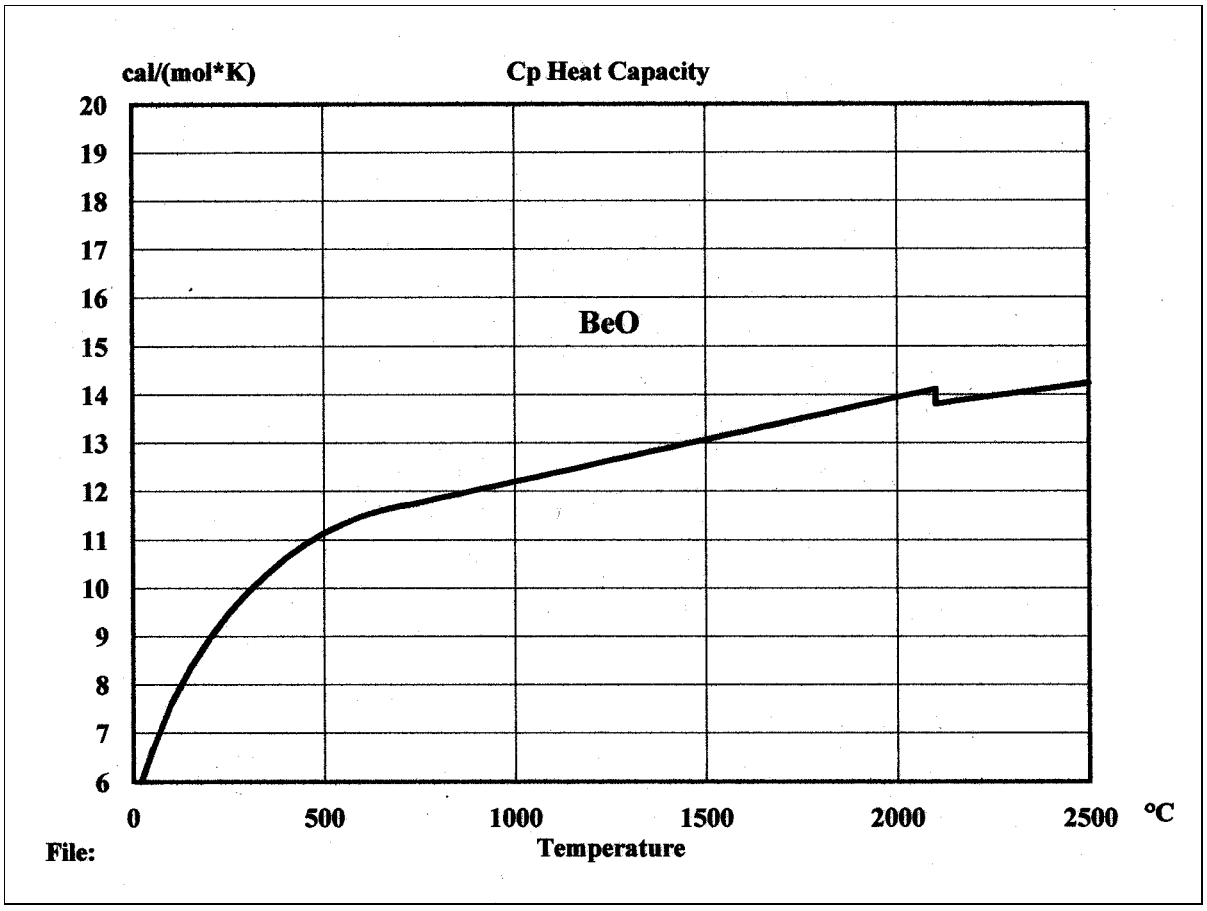

Figure 2.051: Heat capacity of BeO as a function of temperature (90).

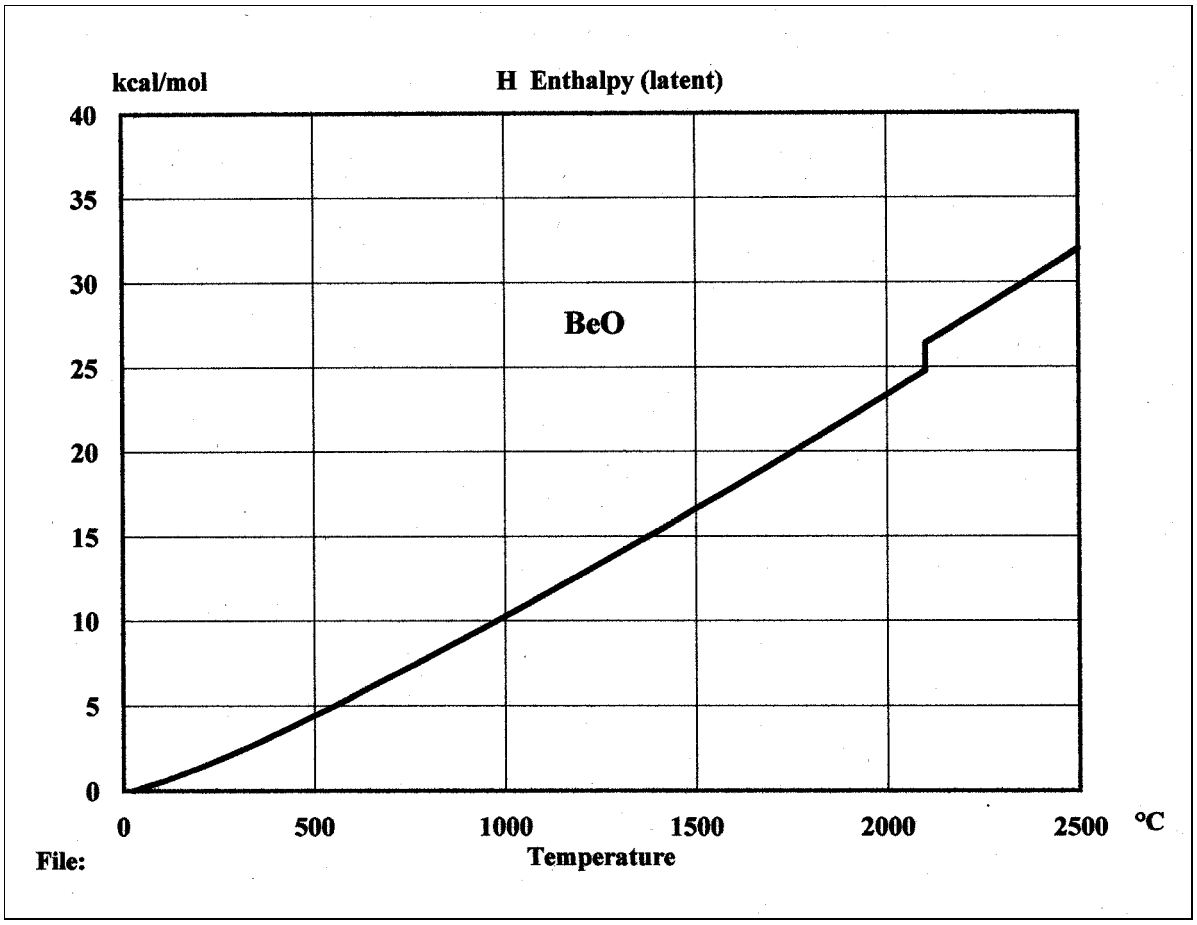

Figure 2.052: Enthalpy of BeO as a function of temperature (90).

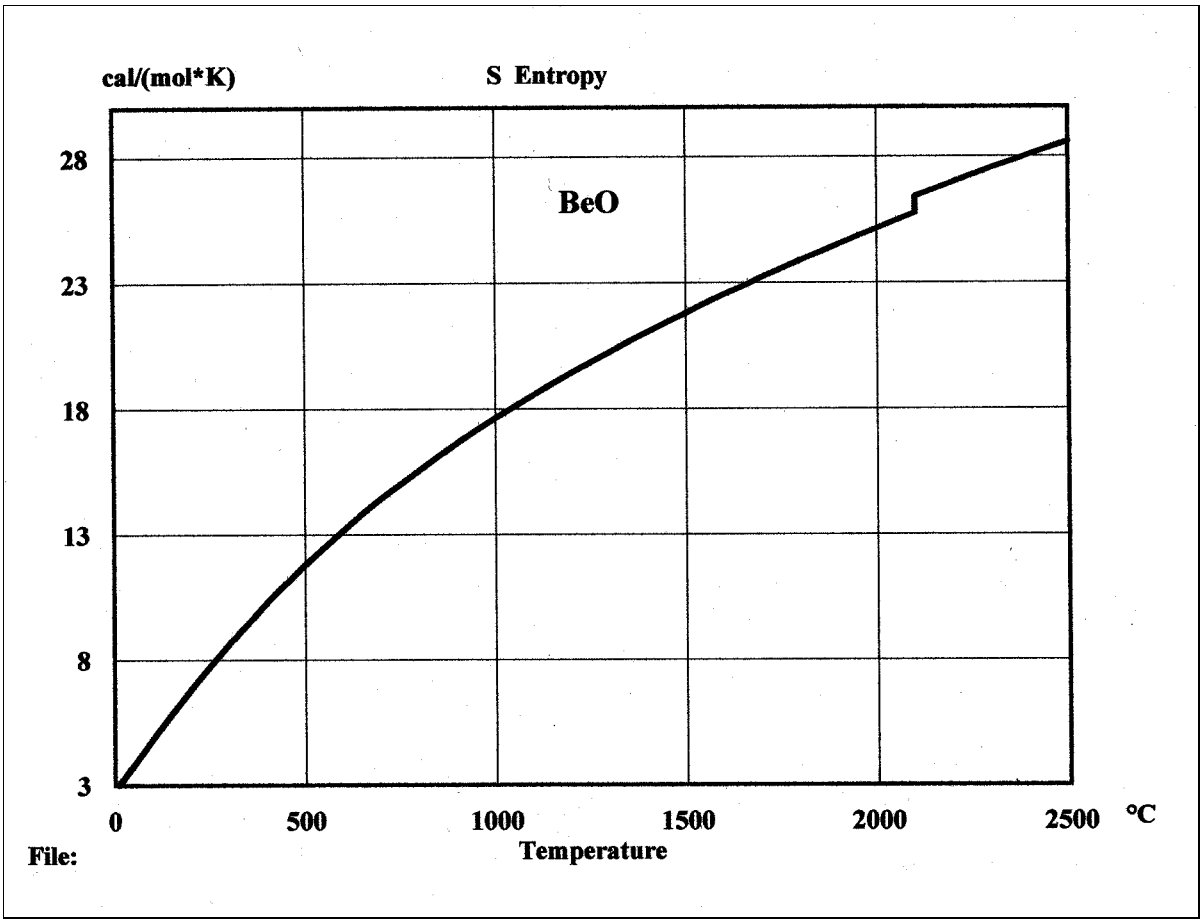

Figure 2.053: Entropy of BeO as a function of temperature (90).

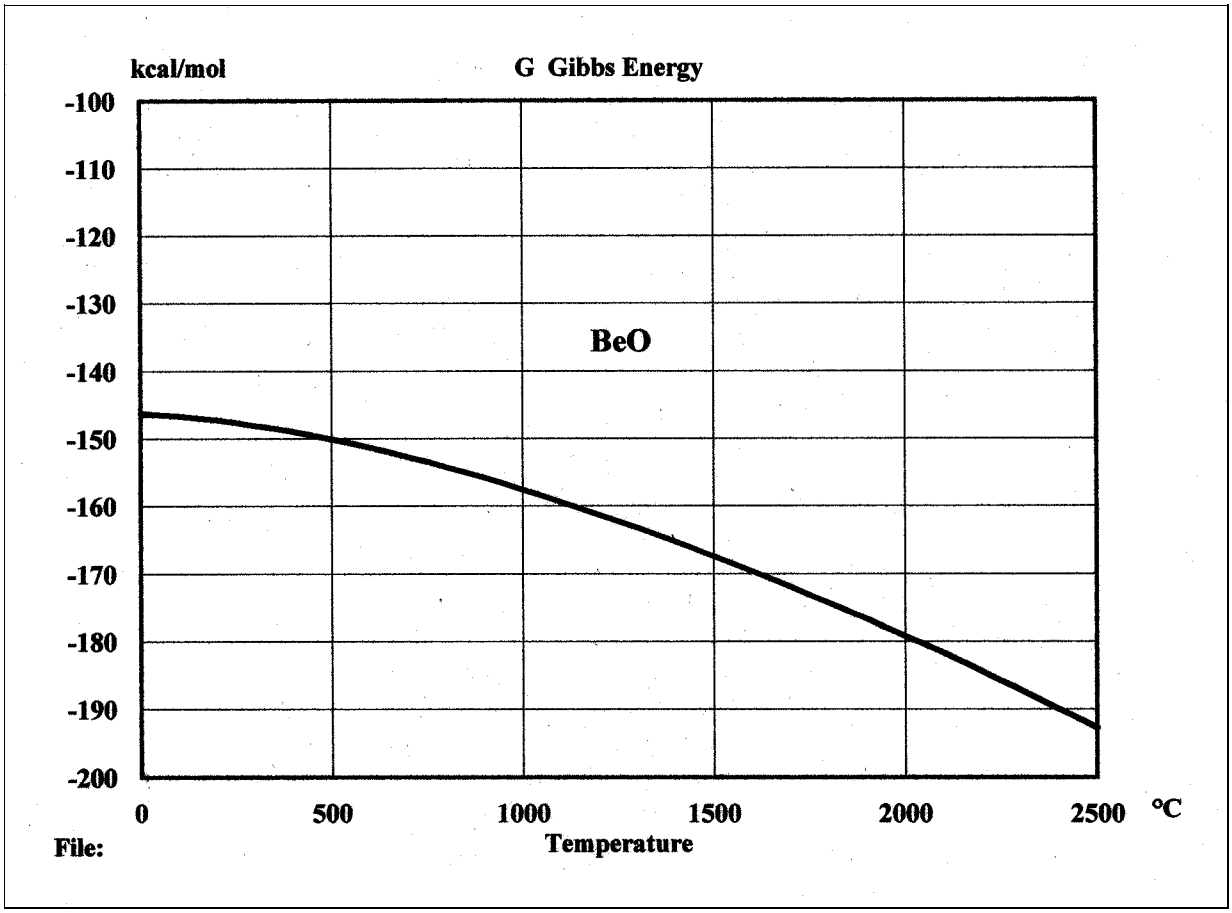

Figure 2.054: Gibbs Free Energy as a function of temperature (90).

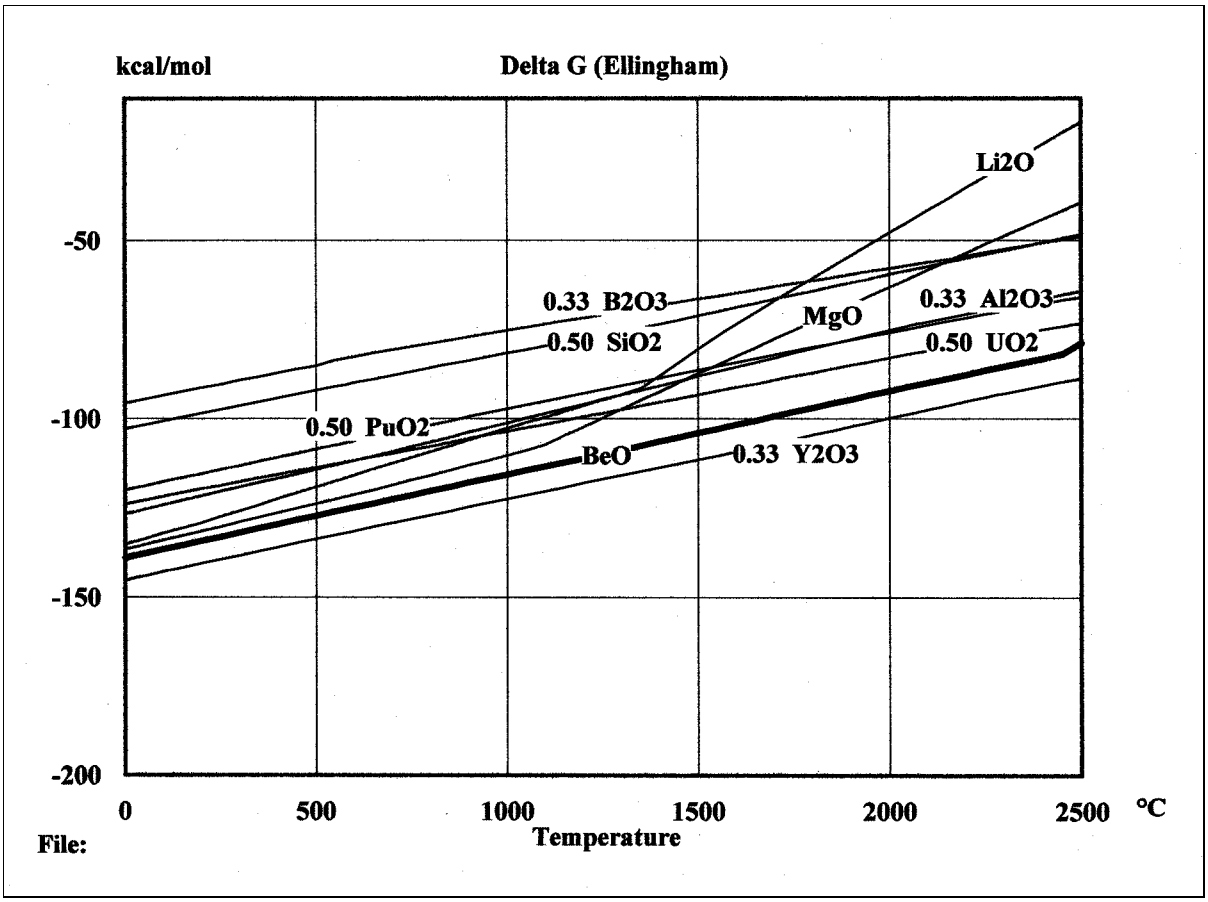

Figure 2.055: Ellingham diagram comparing the stability of BeO to other oxides (90). ΔG values shown are for reactions with ½ mole of O_2. Thus, the reaction for BeO is: Be + ½ O_2 = BeO.

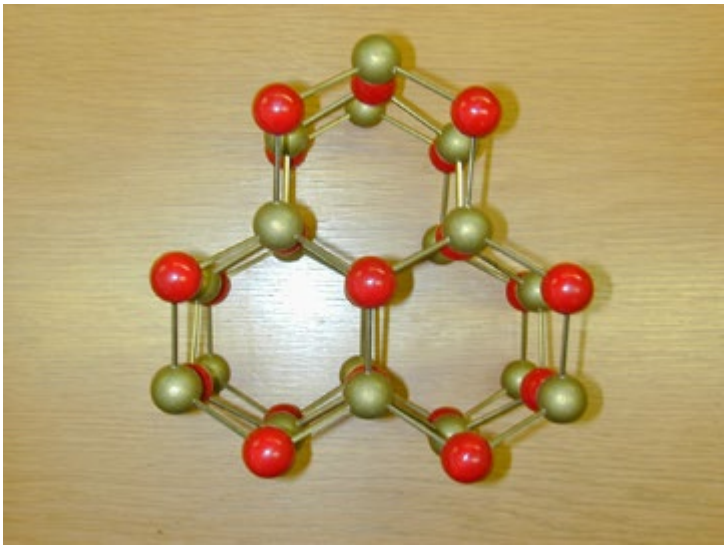

View parallel to the [0001] direction

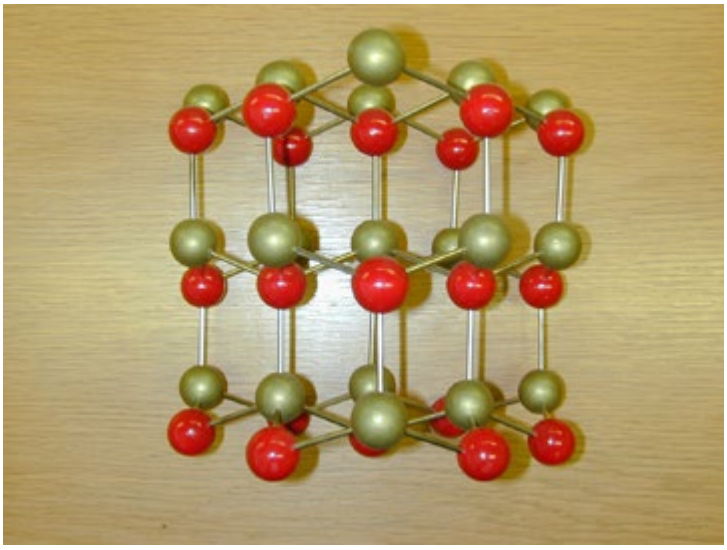

View perpendicular to the [0001] direction

Figure 3.021: Hexagonal crystal structure of BeO.

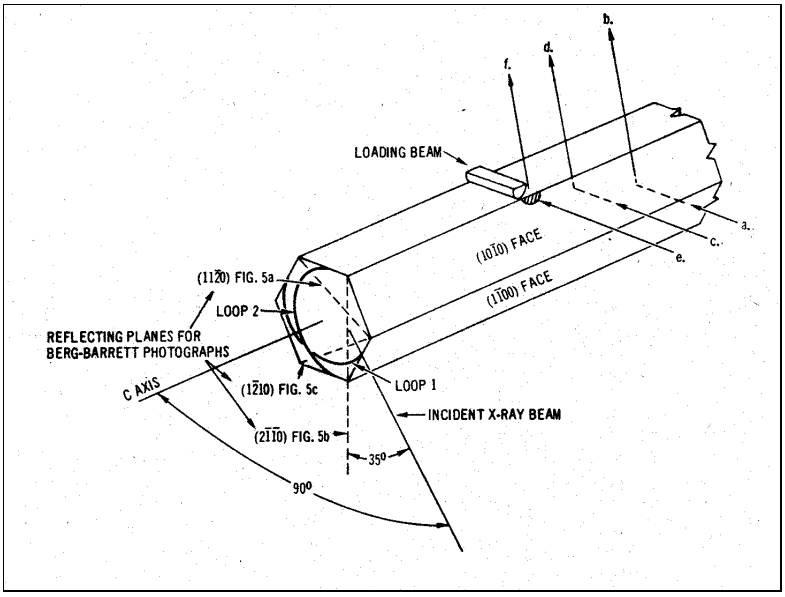

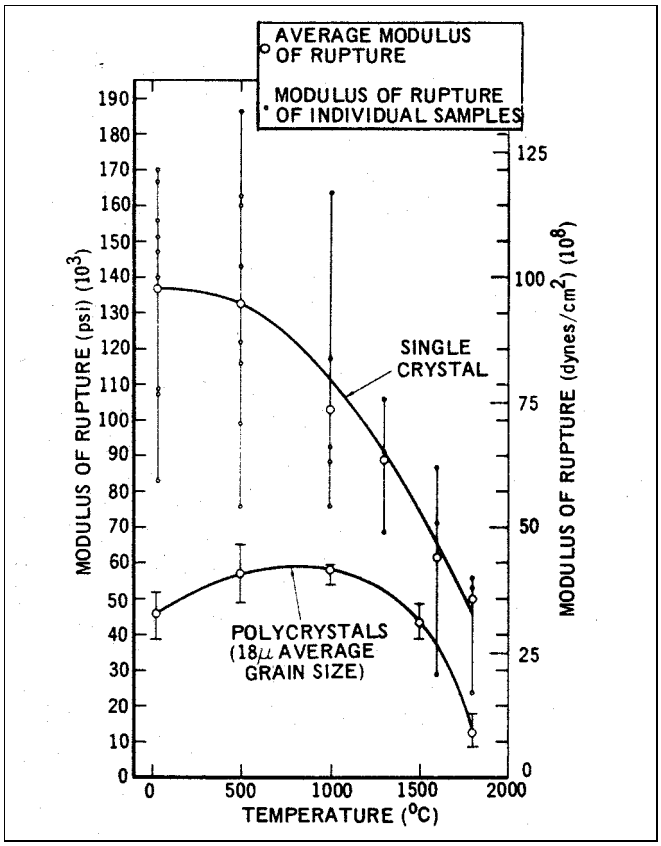

Figure 3.0212: Room temperature three-point bend tests on BeO single crystals (11).

Method	C_{11} (GPa)	C_{12} (GPa)	C_{13} (GPa)	C_{33} (GPa)	C_{44} (GPa)	C_{66} (GPa)	B (GPa)
Ultrasonic (57)	470	168	119	494	153	152	244
Ultrasonic (58)	461	127	89	492	148	167	224
Debye-Waller (59)	460	125	82	490	145	167	222

Figure 3.0213: Room temperature elastic constants of single crystal BeO (57-59).

Grain Size (μm)	Young's Modulus (x 10^6 psi)	Shear Modulus (x 10^6 psi)
2-5	55.1	20.9
7-10	55.8	21.2
15-20	57.1	21.6
35-50	57.3	21.8
60-80	55.9	21.2

Figure 3.0221-1: Young's modulus and shear modulus for fully dense BeO as a function of grain size (12).

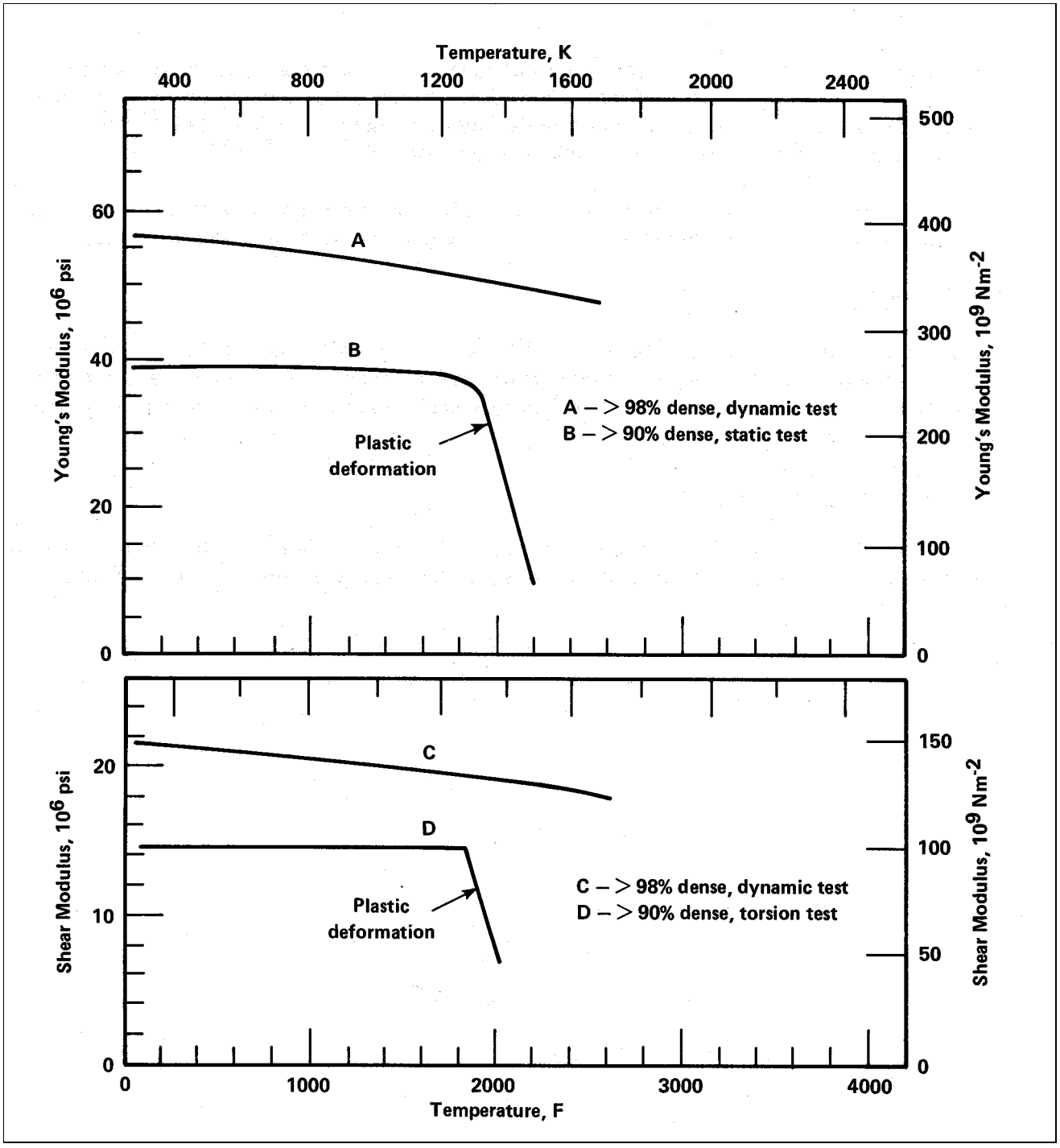

Figure 3.0221-2: Young and shear modulus of BeO as a function of temperature. Curve A and curve C are from Reference 15. Curve B and curve D are from Reference 16.

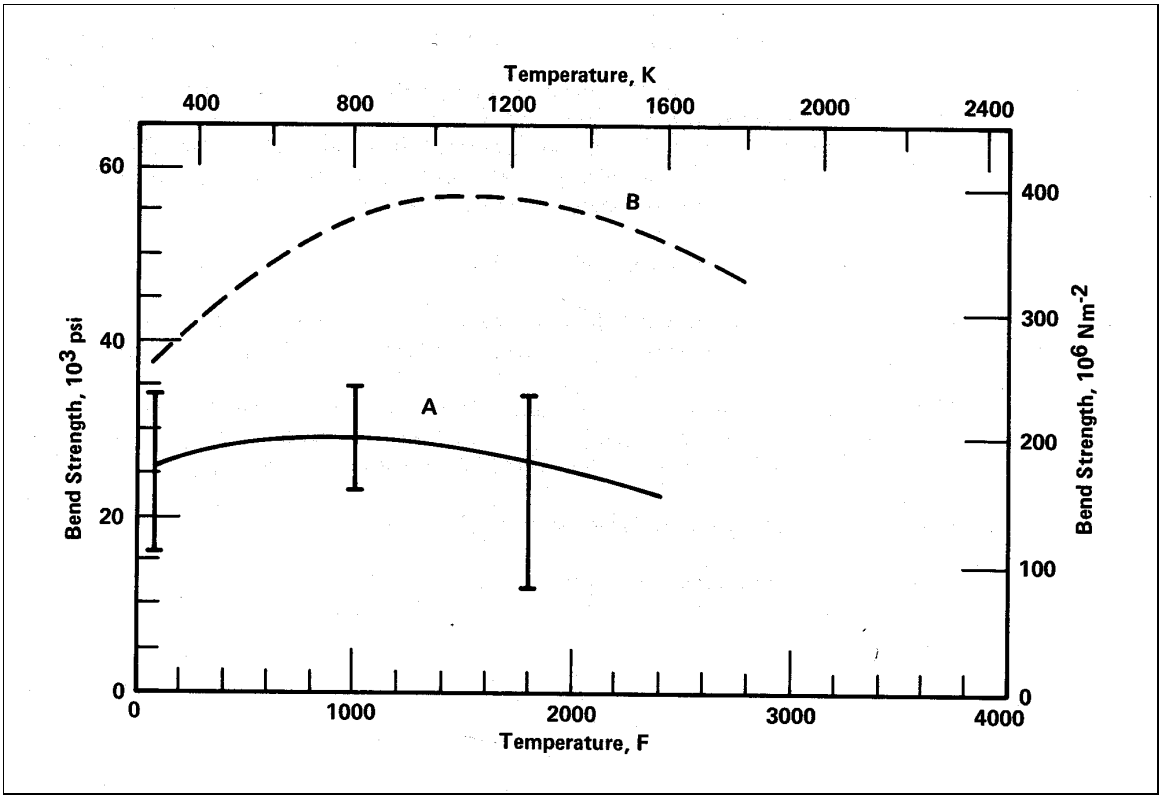

Figure 3.0222: Bend strength of polycrystalline BeO as a function of temperature. Curve A is from Reference 15. Curve B is from Reference 17.

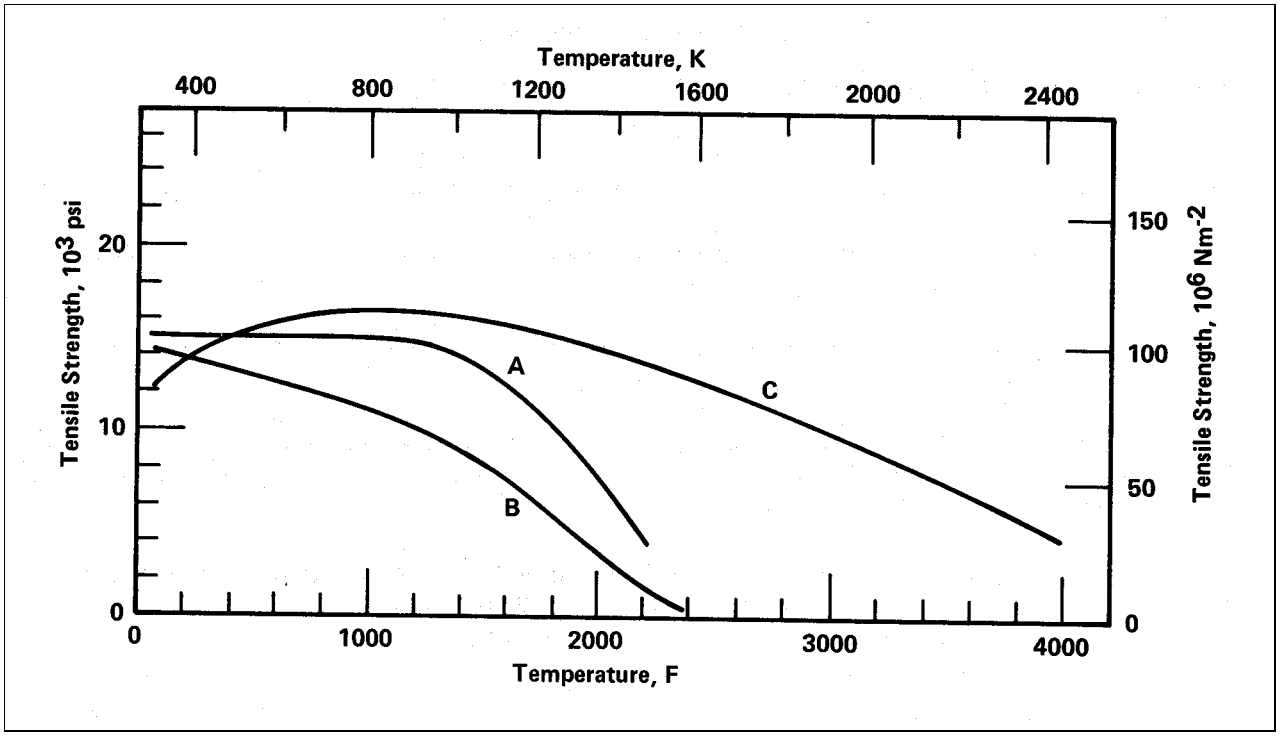

Figure 3.0223: Tensile strength of BeO as a function of temperature. Curve A is from Reference 16. Curve B is from Reference 18. Curve C is from Reference 19.

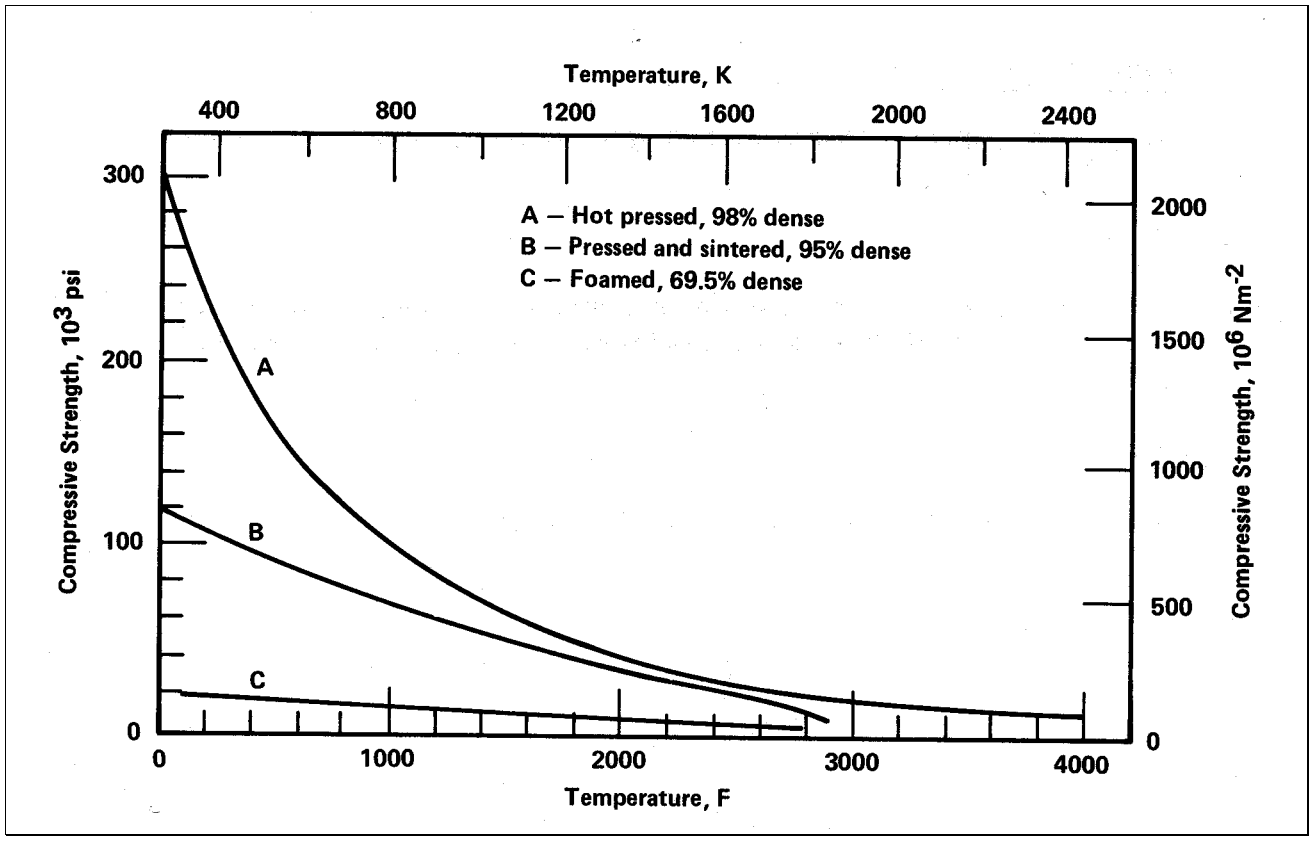

Figure 3.0224: Compressive strength of BeO as a function of temperature. Curve A is from Reference 20. Curve B is from Reference 21. Curve C is from Reference 22.

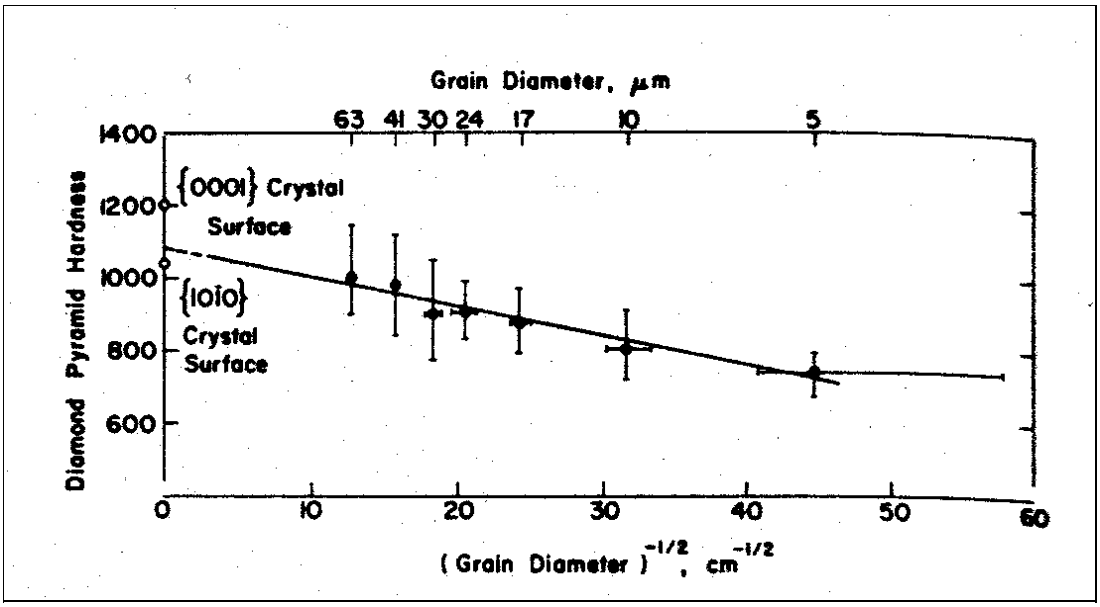

Figure 3.0225: Room temperature Vickers diamond pyramid microhardness of BeO as a function of grain size (23). Microhardness values are in kg/mm^2.

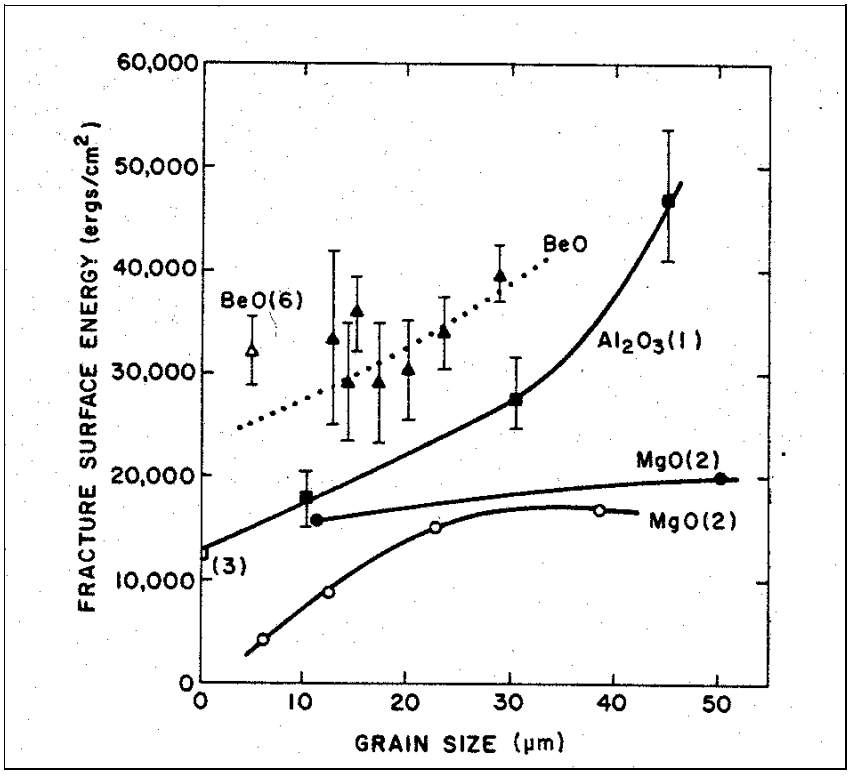

Figure 3.0226: Fracture surface energy of BeO as a function of grain size (24,25).

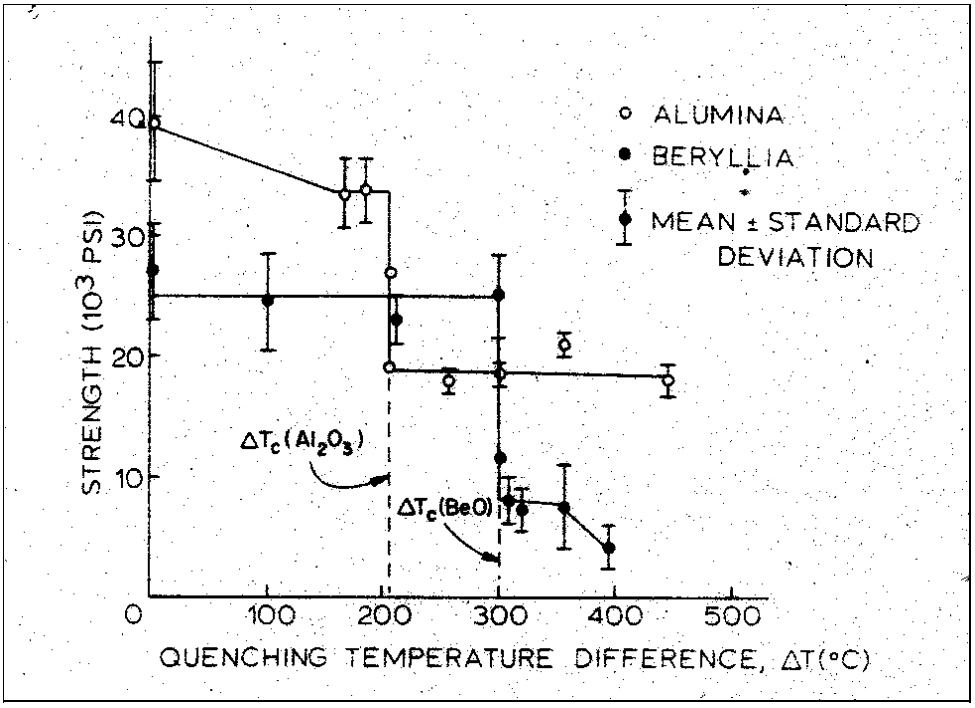

Figure 3.0227: Thermal shock resistance of BeO (27).

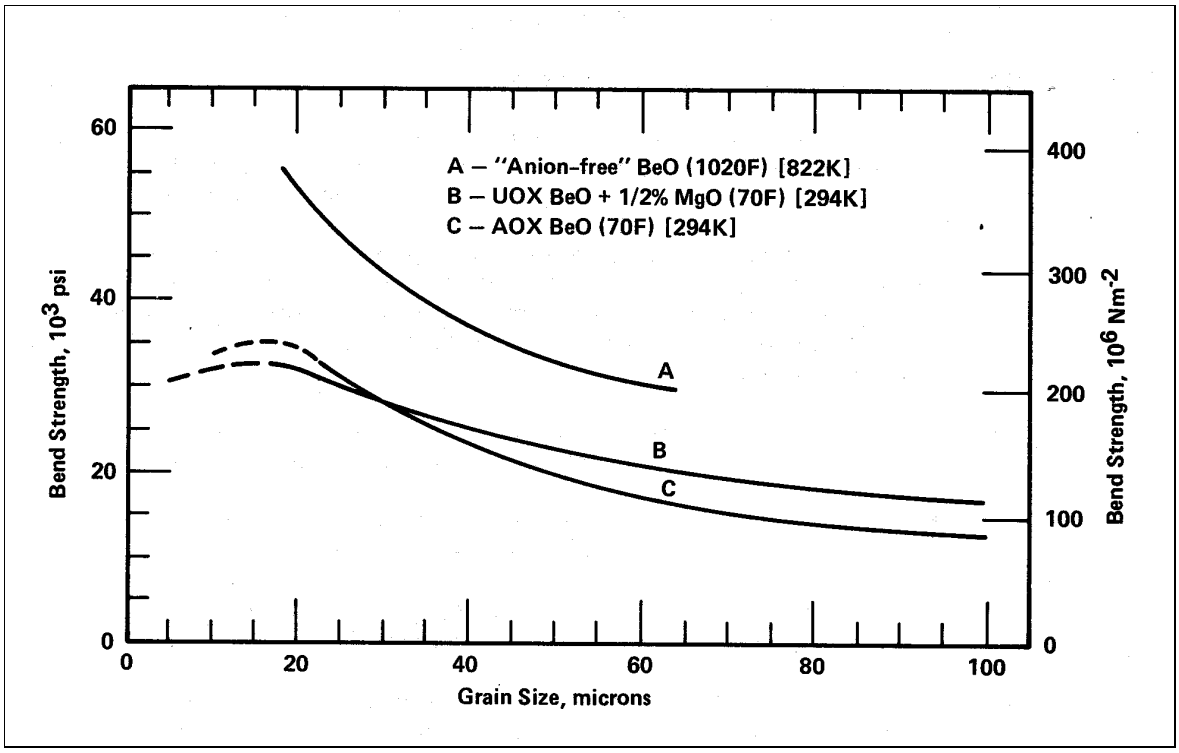

Figure 3.0228-1: Room temperature bend strength of sintered BeO as a function of grain size. Curve B and curve C are from Reference 12. Curve A is for bend tests conducted at 1020 ºF.

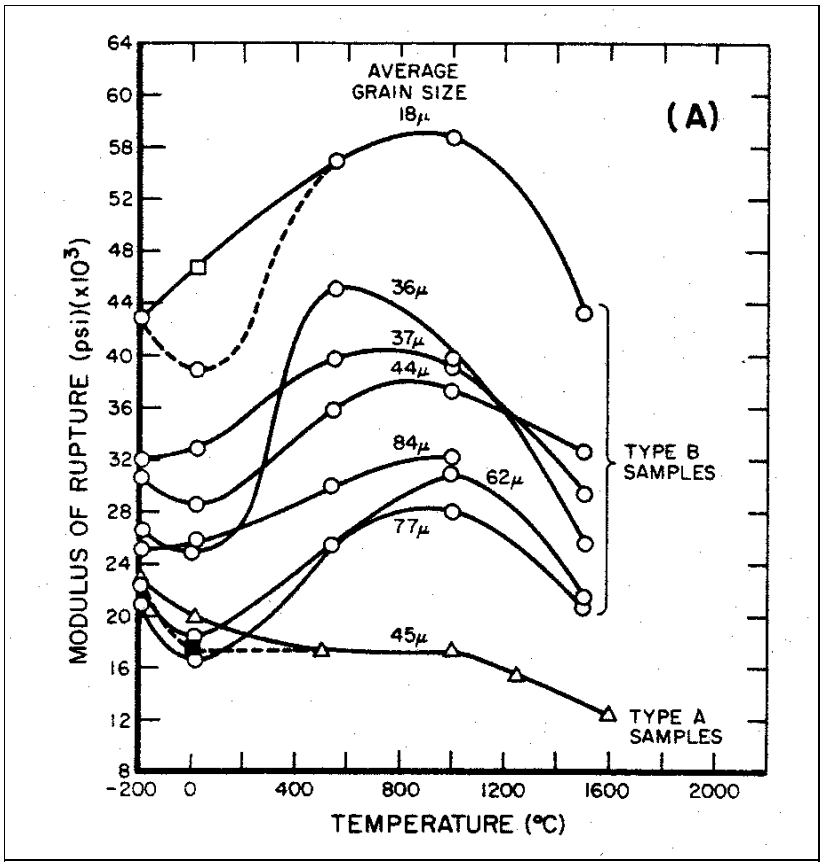

Figure 3.0228-2: Bend strength of hot pressed BeO as a function of grain size and temperature (28).

Table III. Modulus of Rupture of BeO* in Air at Various Strain Rates

Strain rate (in./min.)	Modulus of rupture (avg of 15 tests) (psi)	Standard deviation (psi)
0.0002	22,650	1200
0.020	27,200	1650
0.2	31,400	1400
1.0	30,600	2250

* 99.3% dense, made from The Beryllium Corp. Grade 1 powder.

Figure 3.0229-1: Effect of strain rate on the room temperature bend strength of BeO (28).

Table 4

Effect of Strain Rate on the Modulus of Rupture of BeO in Air

Condition of specimen	*Crosshead speed (in.min⁻¹)*	*No. tested*	*Mean modulus of rupture (p.s.i.)*	*Standard deviation (p.s.i.)*
Machined	0·0025	10	21,520	3,240
	0·050	10	24,170	3,080
	0·010	10	23,830	2,230
	0·500	10	27,350	2,700
	2·000	9	31,610	2,600
Annealed	0·0025	10	26,750	5,090
	0·050	10	32,360	4,390
	0·010	10	32,240	4,860
	0·500	10	43,610	6,840
	2·000	9	39,200	5,310

Table 5

Effect of Strain Rate on the Modulus of Rupture of BeO in Water

Condition of specimen	*Crosshead speed (in.min⁻¹)*	*No. tested*	*Mean modulus of rupture (p.s.i.)*	*Standard deviation (p.s.i.)*
Machined	0·0025	10	21,430	2,590
	0·010	10	21,050	2,540
	0·050	10	19,650	3,190
	0·500	10	26,130	2,810
	2·000	9	29,000	2,360
Annealed	0·0025	10	27,620	4,410
	0·010	10	27,910	5,240
	0·050	10	32,930	3,000
	0·500	9	38,830	5,320
	2·00	8	41,730	4,160

Figure 3.0229-2: Effects of strain rate on BeO room temperature bend strength in both air and water (29).

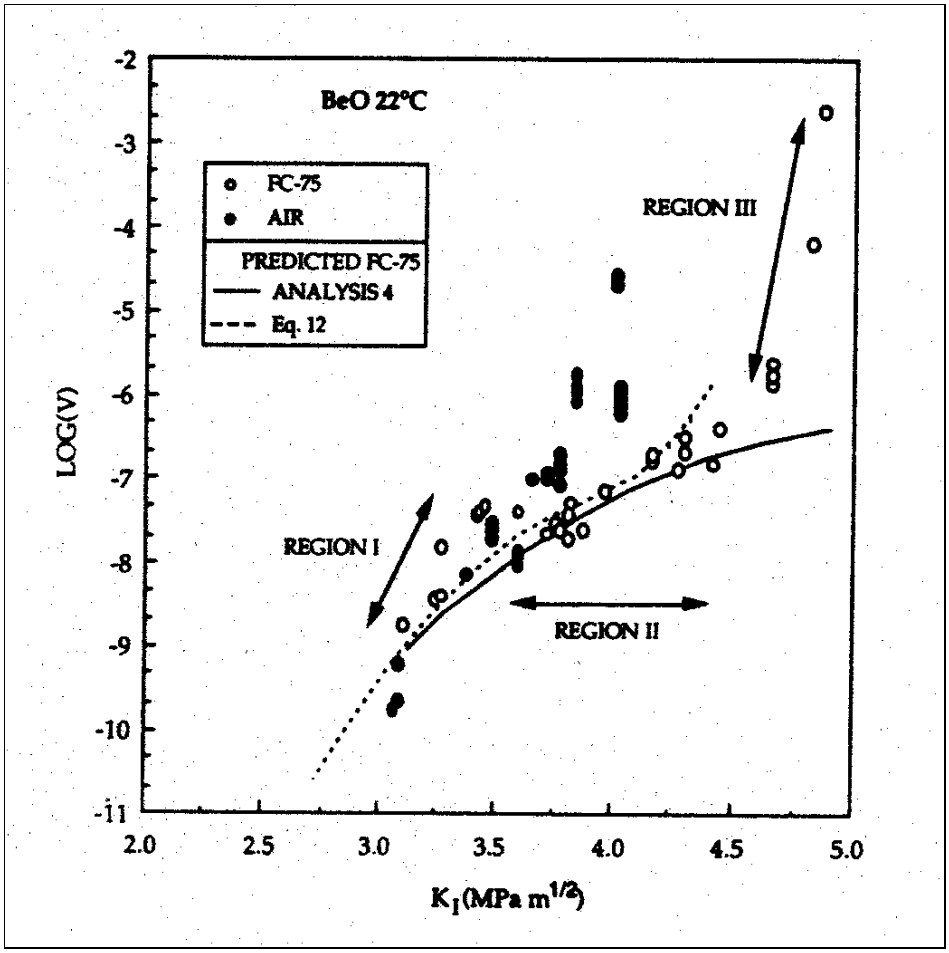

Figure 3.0229-3: Crack velocity versus stress intensity factor K_I for notched bend tests in a fluorocarbon fluid equivalent to an environment of air at 68% relative humidity (30).

Table 1
Effect of Machining on the Strength of As-sintered Extruded Rods

Batch No.	*No. tested*	*Condition*	*Mean modulus of rupture (p.s.i.)*	*Standard deviation (p.s.i.)*
A	40	As sintered	30,500	6,200
	40	Machined	24,700	5,100
B	14	As sintered	35,350	4,100
	14	Machined	33,500	4,600
C	10	As sintered	34,600	6,000
	10	Machined	20,500	2,200
		Machined, then annealed 4 h at 800°C in air	31,000	
D	15	As sintered	33,000	3,300
		Machined	24,900	2,470

Table 2
Effects of Annealing Machined Extruded Rods

No.	*Condition of specimen*	*Number tested*	*Mean modulus of rupture (p.s.i.)*	*Standard deviation (p.s.i.)*
1	As machined	11	22,900	1,770
2	After annealing in air at 800°C for 1 h	10	32,900	4,310
3	As 2, for 2 h	10	30,000	3,490
4	As 2, for 4 h	10	31,500	2,000
5	As 2, for 8 h	10	34,400	3,420
6	As 2, for 16 h	12	32,500	3,560
7	After annealing in air at 800°C for 16 h, then re-machining	9	21,500	3,750
8	As 7, then re-annealed 16 h at 800°C in air	8	30,300	4,800

Crosshead speed: 0·05 in.min^{-1}
Test atmosphere: air

Figure 3.02210: Effects of machining on the strength of BeO (29). Note that the strength of machined BeO increases if the material is annealed to relieve machining stresses.

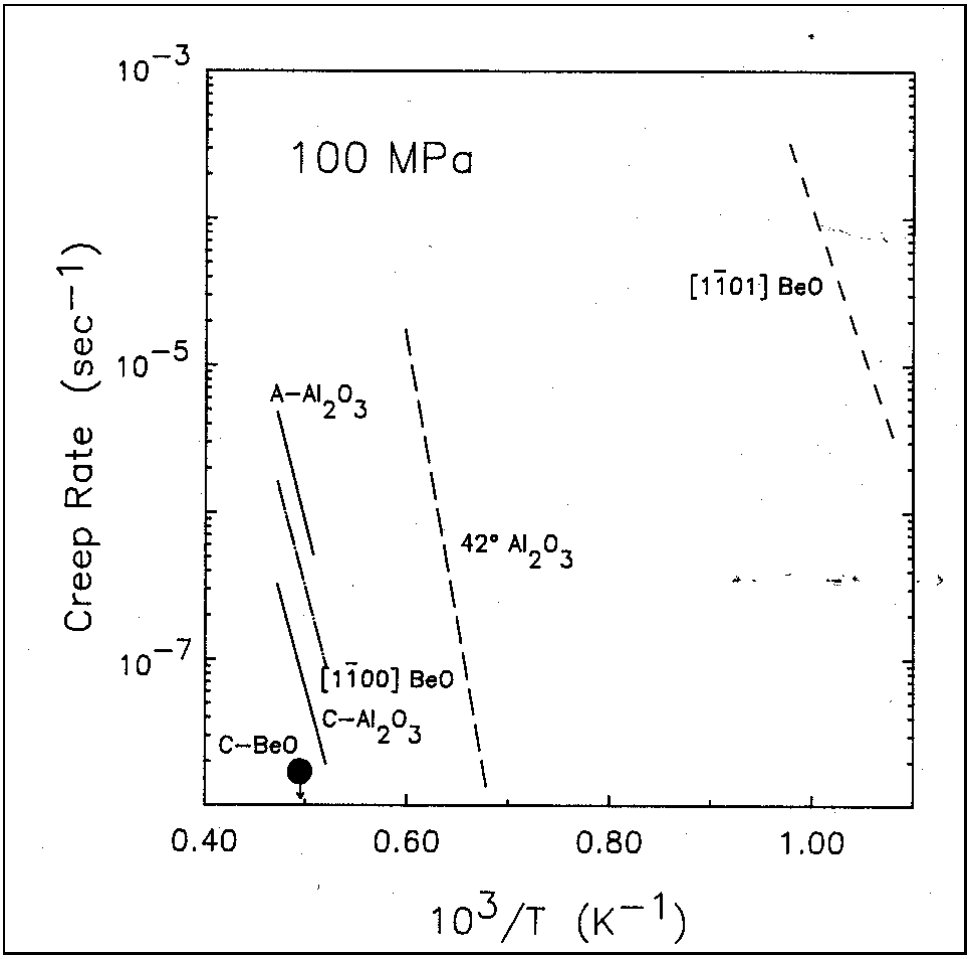

Figure 3.02211-1: Creep rate versus temperature for single crystal BeO (37). The applied stress is 100 MPa. The BeO data is compared to that of single crystal Al_2O_3.

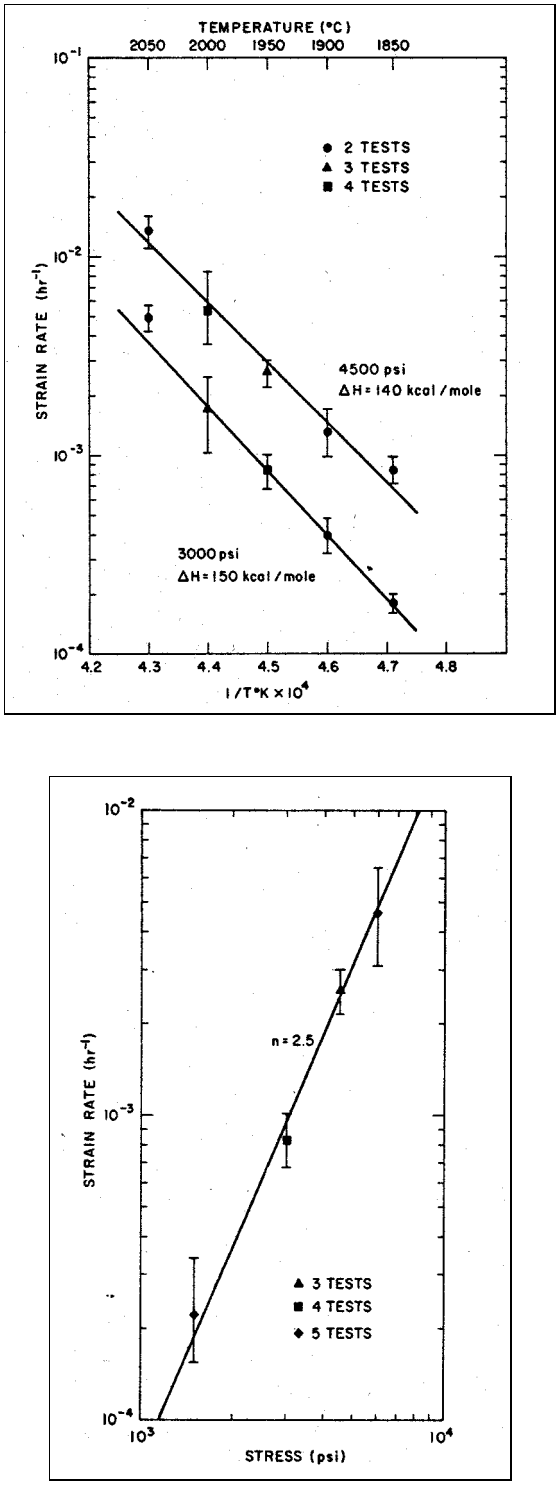

Figure 3.02211-2: Effects of temperature and stress level on the creep of polycrystalline BeO (35).

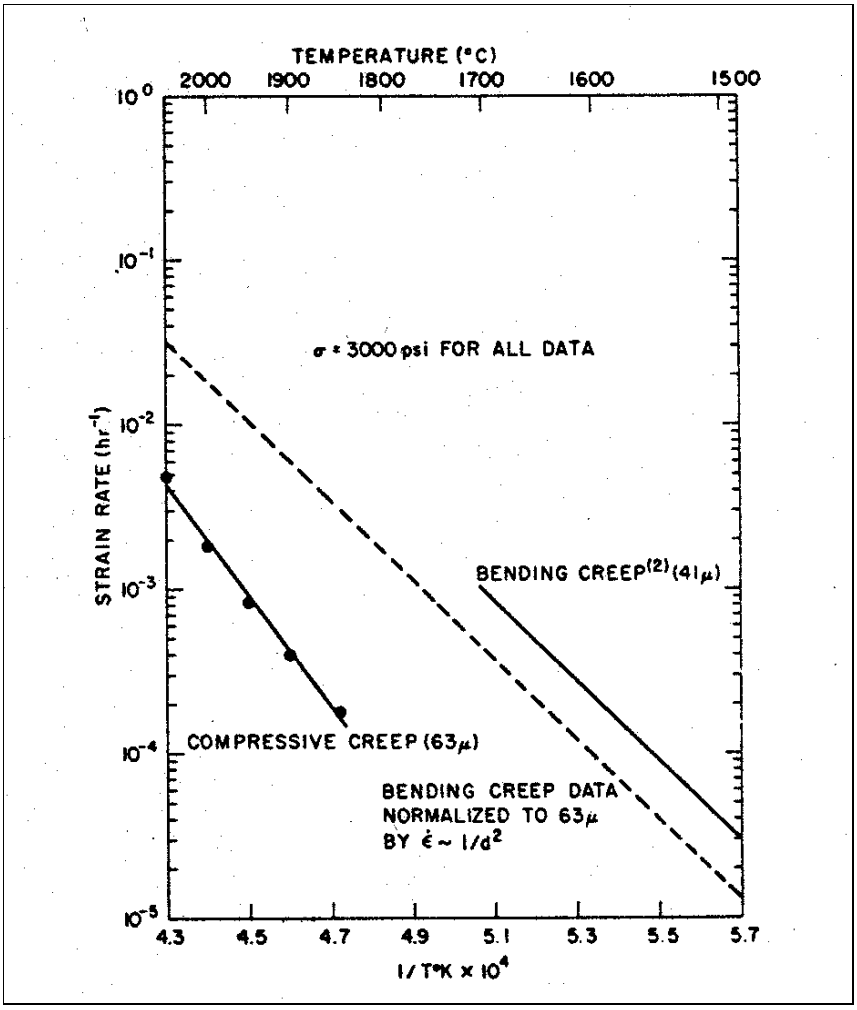

Figure 3.02211-3: Comparison of the creep rate of BeO in compression and bending (35).

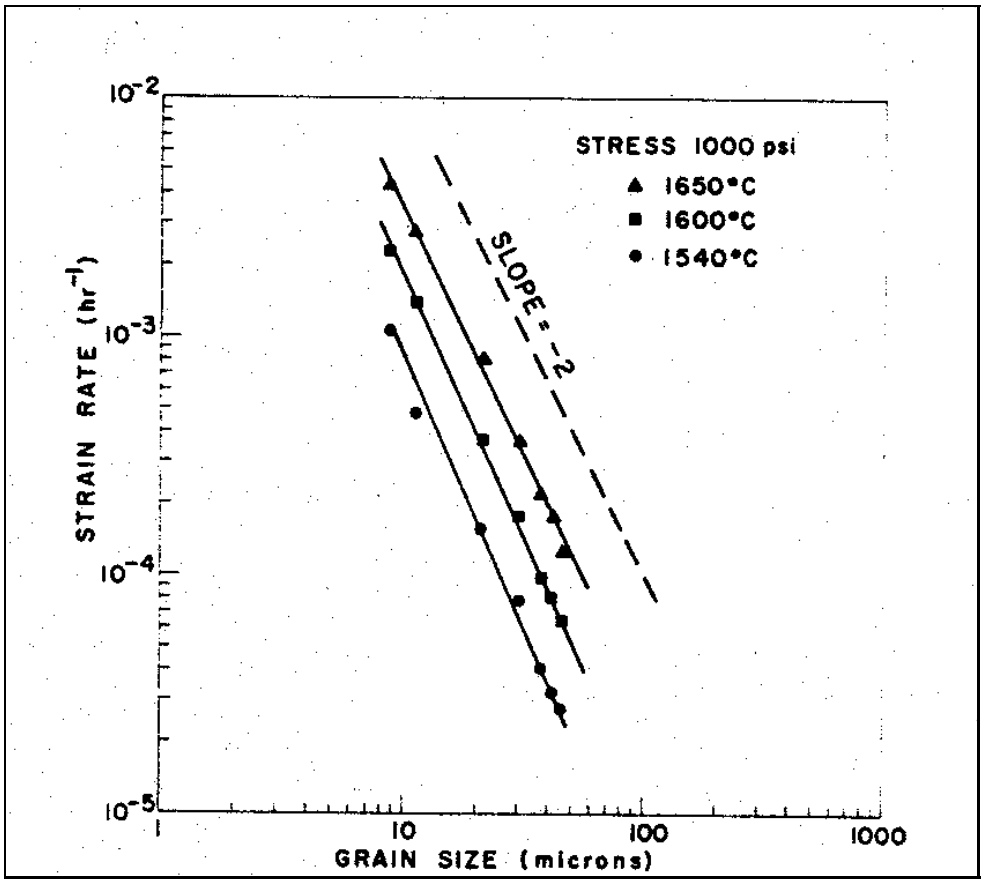

Figure 3.02211-4: Grain size effects on the creep rate of polycrystalline BeO (34).

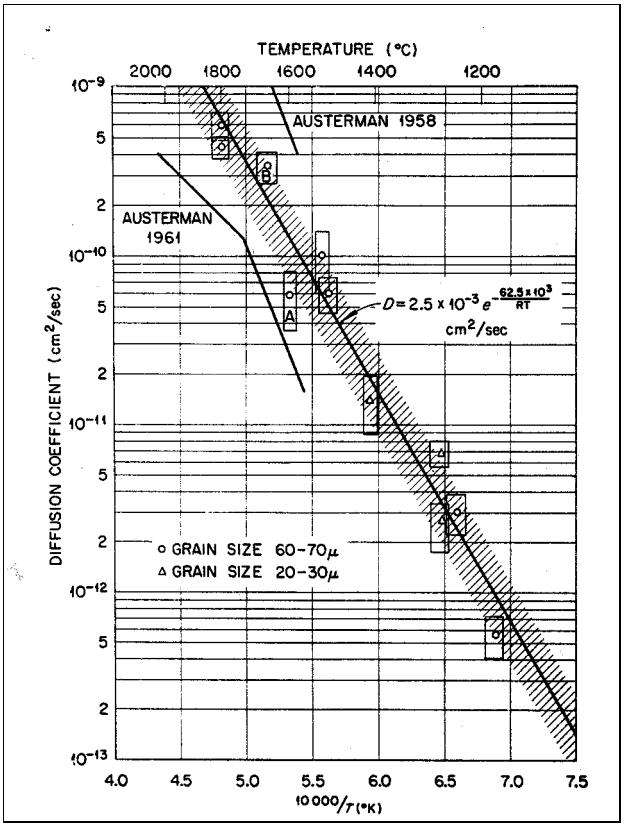

Beryllium diffusion

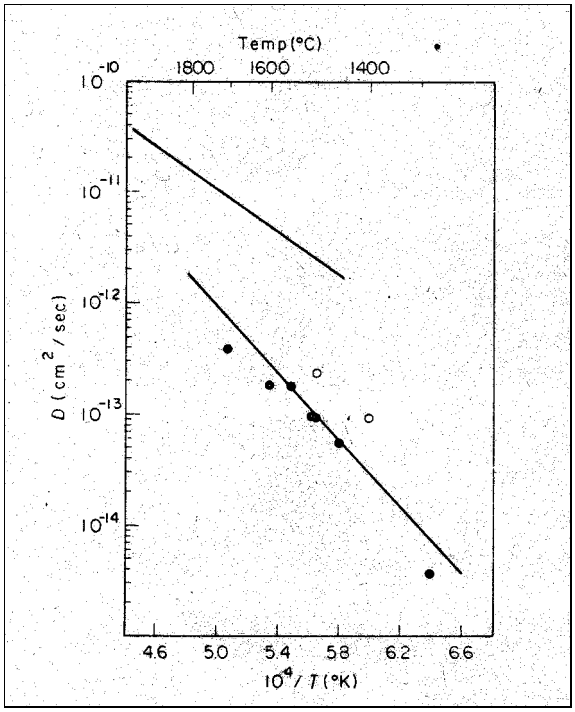

Oxygen diffusion

Figure 3.02212: Self-diffusion coefficients of beryllium (38) and oxygen (39) in BeO.

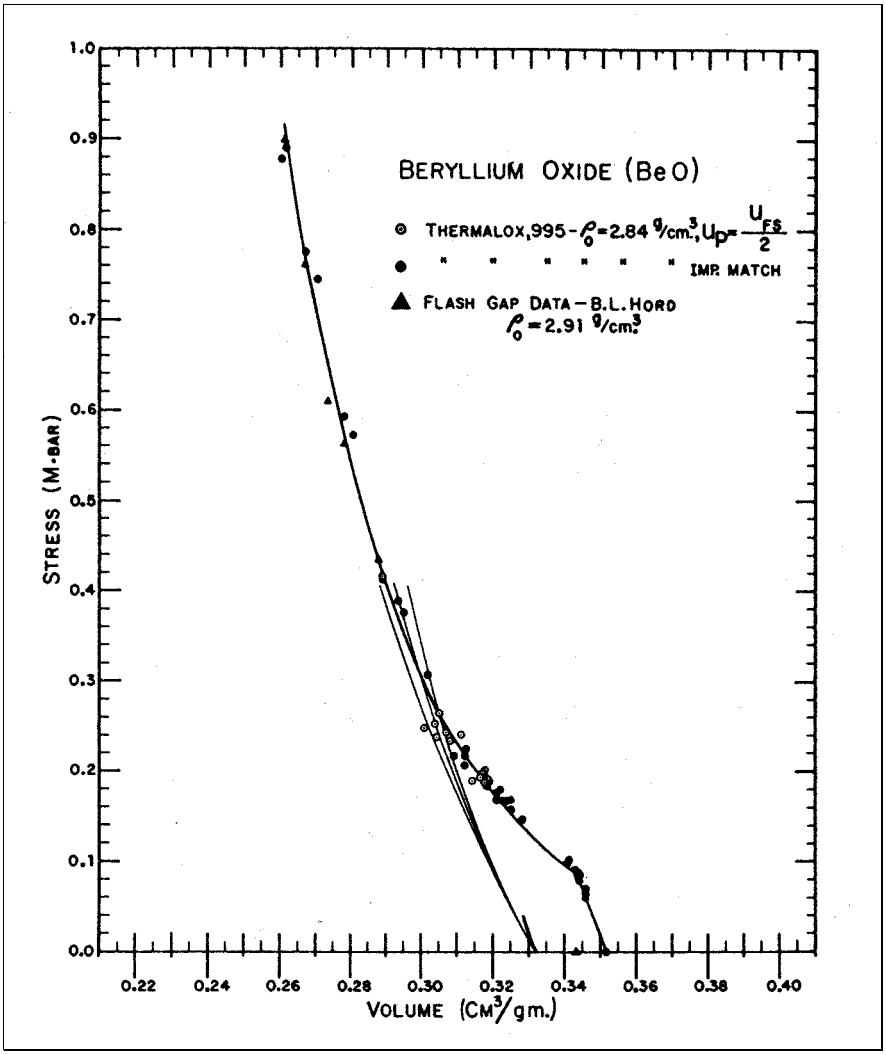

Figure 3.02213-1: Hugoniot for BeO of initial density 2.84 g/cm^3 (72).

BERYLLIUM OXIDE, ρ_0 = 3.0 g/cm^3.

Average ρ_0 = 2.989 g/cm^3.

Sound velocities longitudinal 11.91 km/s.
shear 7.28 km/s.

Reference 33

ρ_0 (g/cm^3)	U_s (km/s)	U_p (km/s)	P (GPa)	V (cm^3/g)	ρ (g/cm^3)	V/Vo	Exp	
2.989	8.437	0.000	0.000	.3346	2.989	1.000	ssp	×
2.992	10.540	.317	9.997	.3242	3.085	.970	iml	o
2.991	10.543	.458	14.443	.3198	3.127	.957	iml	o
2.991	10.344	.664	20.543	.3129	3.196	.936	iml	o
2.991	10.086	.939	28.327	.3032	3.298	.907	iml	o
2.990	10.339	1.361	42.073	.2904	3.443	.868	iml	o
2.990	10.439	1.522	47.506	.2857	3.500	.854	iml	o
2.986	10.512	1.825	57.285	.2768	3.613	.826	iml	o
2.986	11.165	2.268	75.612	.2669	3.747	.797	iml	o
2.986	11.284	2.412	81.270	.2633	3.798	.786	iml	o
2.989	12.054	2.822	101.675	.2562	3.903	.766	iml	o

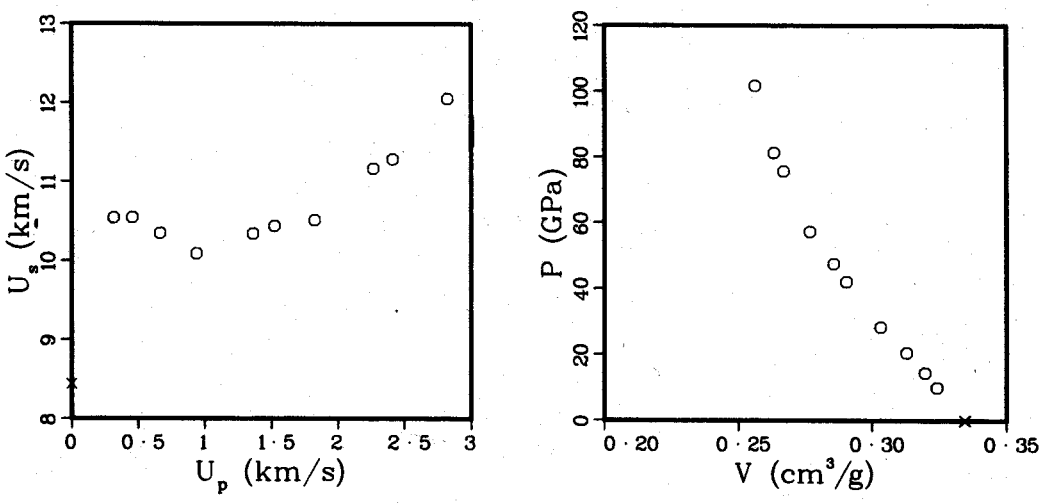

Figure 3.02213-2: Hugoniot for BeO with an initial density of 3.0 g/cm^3 (73).

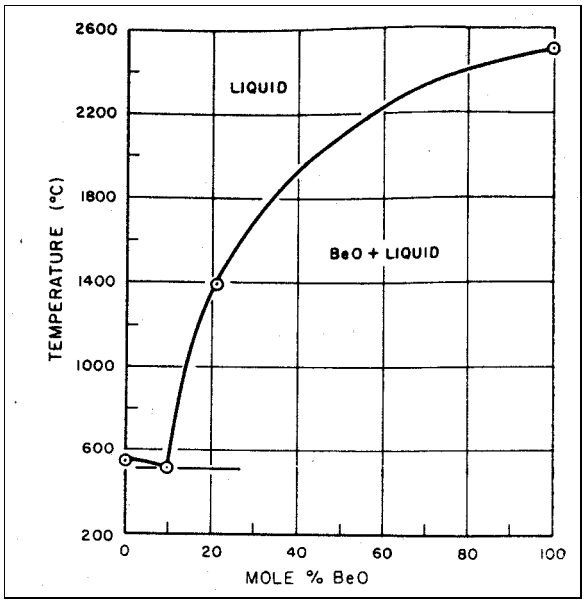

Figure 4.01-1: Approximate liquidus diagram of the system Li_2MoO_4-1.25 MoO_3-BeO (42).

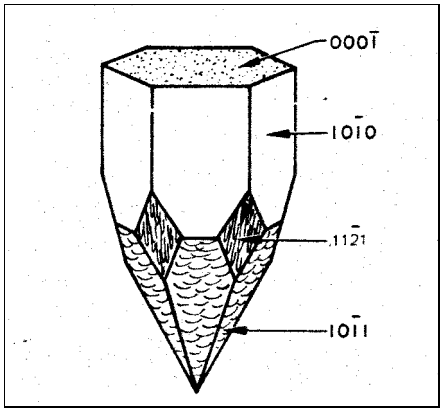

Figure 4.01-2: Sketch of BeO single crystal (43).

Table II
UOX and GC-HF Powder Characteristics

	UOX		GC-HF	
	Typical	Maximum	Typical	Maximum
Loss on Drying, %	0.3	1.0	0.03	0.15
Loss on Ignition After Drying, %	0.5	1.0	0.03	0.15
Density, g/cc				
Bulk	0.20		0.35	
Tap	0.35		0.67	
Particle Size Cumulative Percent Finer Than				
20 µm	99		98	
14 µm	98		97	
8 µm	90		90	
4 µm	65		35	
1 µm	25		2	
Surface Area, m^2/g	9-12		1-2	

TABLE I
Chemical Composition of UOX and GC-HF Beryllium Oxide Powders

		UOX		GC-HF	
Element	Content Units	Typical	Maximum	Typical	Maximum
Sulfur	%	0.08	0.15	0.02	0.06
Aluminum	ppm	40	100	40	100
Calcium	ppm	<30	50	<30	50
Iron	ppm	20	50	20	50
Magnesium	ppm	25	50	25	50
Silicon	ppm	50	100	50	100
Sodium	ppm	25	50	25	50
Boron	ppm	<1	3	<1	3
Cadmium	ppm	<1	2	<1	2
Chromium	ppm	5	10	5	10
Cobalt	ppm	<1	3	<1	3
Copper	ppm	<2	5	<2	5
Lead	ppm	<2	5	<2	5
Lithium	ppm	<1	3	<1	3
Manganese	ppm	2	5	2	5
Molybdenum	ppm	<3	5	<3	5
Nickel	ppm	<3	10	3	10
Silver	ppm	<1	3	<1	3
BeO		Balance		Balance	

Figure 4.021: Specifications on Materion BeO powder.

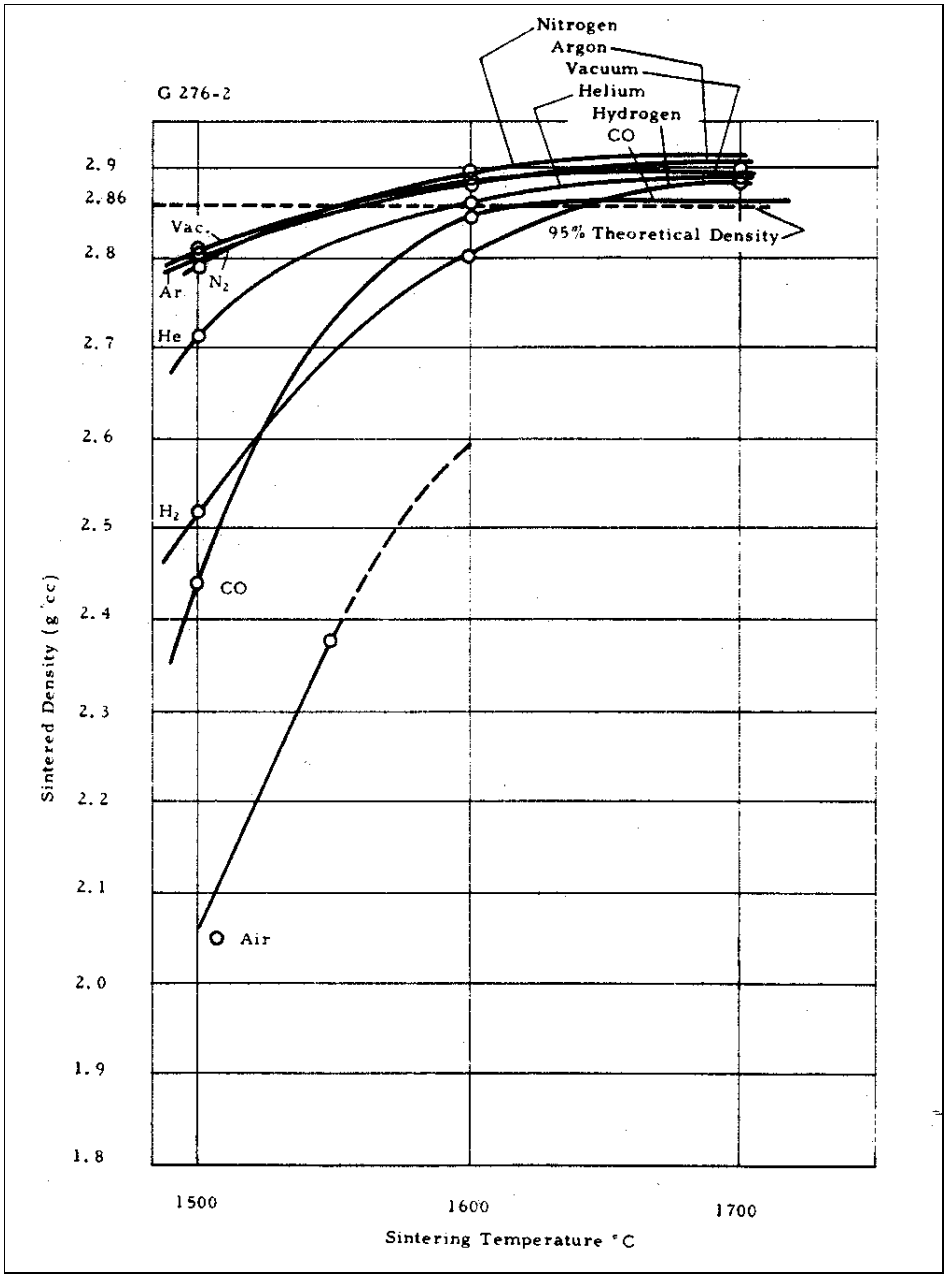

Figure 4.0221-1: Sintering behavior of BeO as a function of sintering temperature and sintering atmosphere (51). The sintering time was 3 hours.

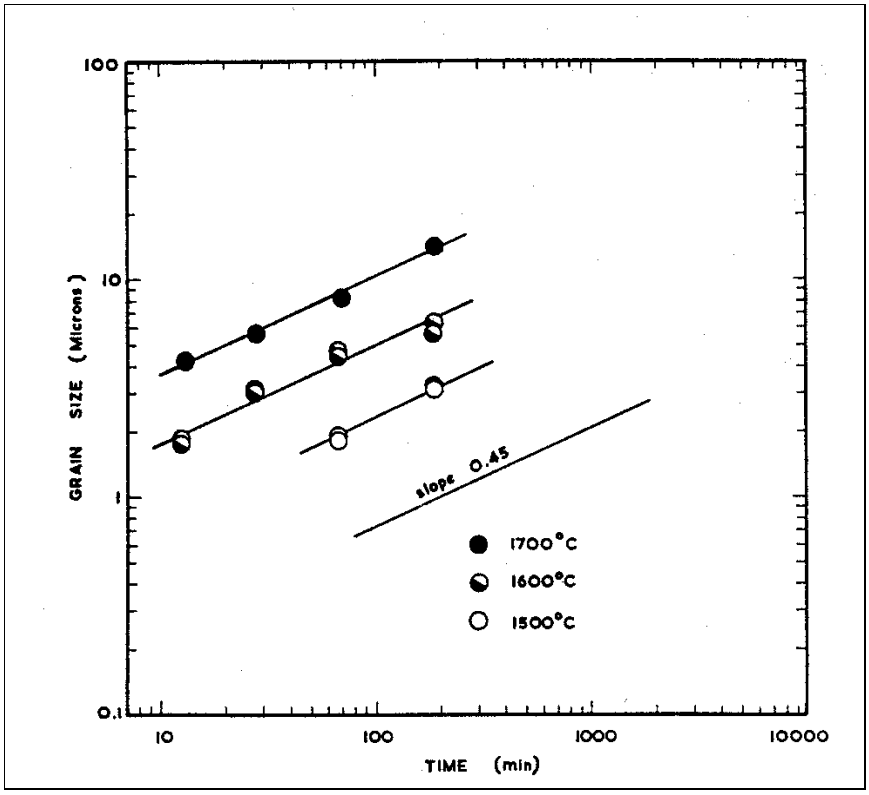

Figure 4.0221-2: Grain growth occurring during the sintering of BeO (48).

Analyses of Raw BeO Powders* (ppm)

	Powder "A"	Powder "B"	Powder "C"	Powder "D"
Al	< 100	200	< 100	75
Ca	100	100	75	80
Cu	5	< 5	10	1
Fe	< 100	200	100	35
Mg	75	100	25	50
Mn	< 20	35	20	1
Mo	< 10	5	10	< 3
Na	< 25	< 25	35	75
Ni	< 20	75	< 20	7
Pb	< 5	5	5	< 2
Si	450	350	500	25
Ti	< 50	< 50	< 50	1
Zn	< 100	< 100	< 100	< 30
Oxide Purity, %	99.9	99.9	99.9	99.95
F	ND	5–8000	ND	20
P	ND	200	ND	ND
S	1–3000	ND	3–500	30

* Not necessarily typical of commercial grade. "ND" = "not determined".

BeO end-point density *vs* pressing temperature (@ 2000 psi)

Temperature °C	Density in % of theoretical			
	Powder "A"	Powder "B"	Powder "C"	Powder "D"
1700	99.5	99.5	99	99
1500	96	95	84	
1300	92	94	76	73
1100	84	78	64	

Figure 4.023-1: Hot pressing densification as a function of temperature four different purities of BeO powder (63).

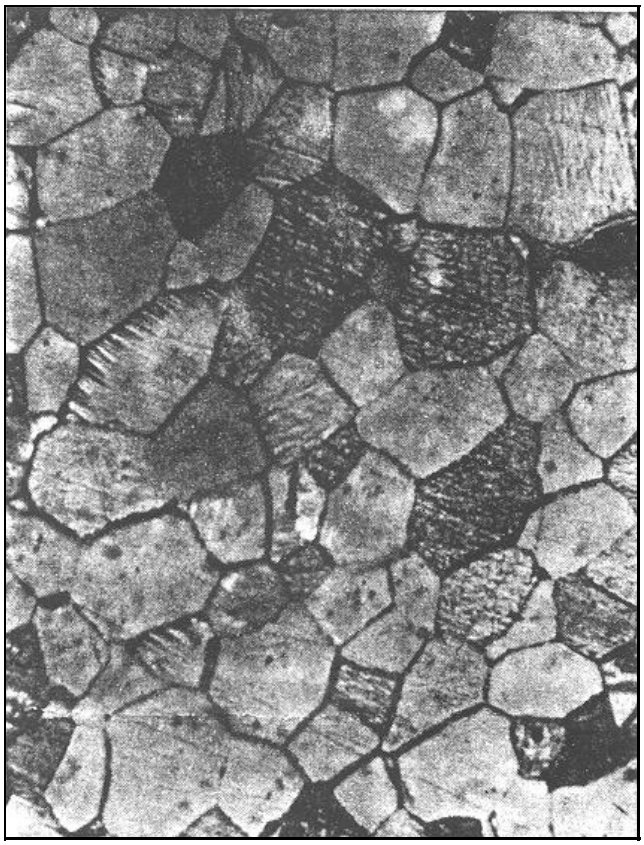

Figure 4.023-2: Micrograph showing grain size and structure of BeO consolidated to 99.5% density by hot pressing of high purity “D” powder at 1700 ºC (63).

EFFECT OF TEMPERATURE, PRESSURE, AND TIME

ON THE POROSITY OF HOT PRESSED BeO

HOT PRESSING TECHNIQUE						Bulk Porosity per cent
Fixed Parameters			Varied Parameter			
Temp. (°C)	Press. (kg/cm^2)	Time (min.)	Temp. (°C)	Press. (kg/cm^2)	Time (min.)	
		-	-	-	1	6.0
		-	-	-	3	3.5
		-	-	-	5	1.7
1500	250	-	-	-	10	1.0
		-	-	-	25	0.7
		-	-	-	50	0.65
		-	-	-	100	0.7
	-		-	100	-	5.0
	-		-	150	-	1.6
1500	-	25	-	200	-	1.2
	-		-	250	-	0.75
	-		-	300	-	0.60
-			1300	-	-	5.0
-			1400	-	-	2.0
-	250	25	1500	-	-	0.7
-			1600	-	-	0.5
-			1700	-	-	0.3

Figure 4.023-3: Effects of temperature, pressure, and time on the residual porosity left in hot pressed BeO material (67).

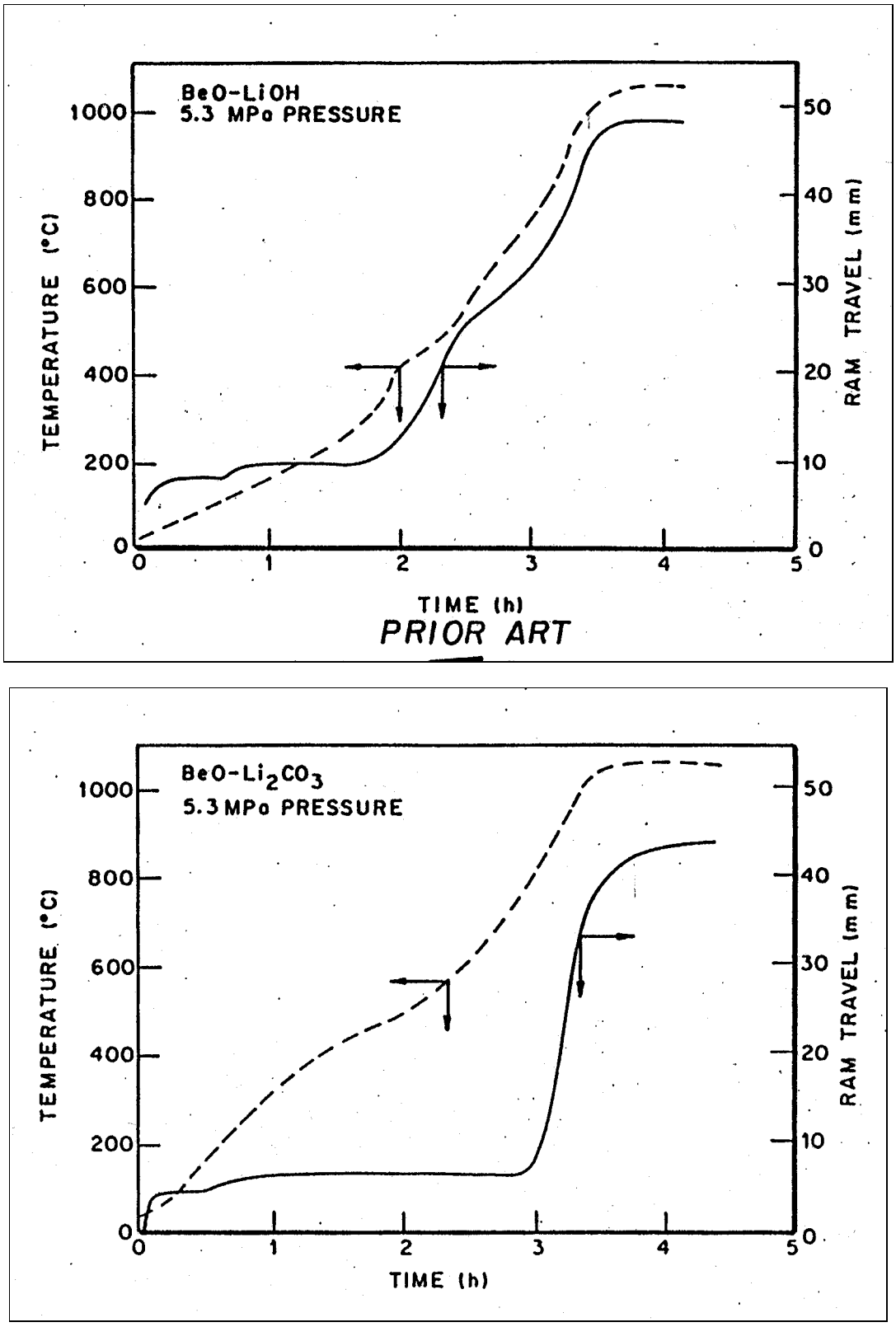

Figure 4.023-4: Effects of lithium-based densification aids on the hot pressing of BeO (71).

Table 1. Characteristics of BeO after the hot isostatic pressing at 2 kbars.

Sample No.	Temperature (°C)	Run duration (min)	Relative density (%)	Grain size (μ)	Remarks
1	1000	5	96.4	0.8	light gray
2	1000	20	99.7	1	white color; strongly bonded with platinum foil
3	1000	60	99.9	2	light gray
4	1000	150	99.9	2.5	slightly translucent
5	1200	5	99.0	2.5	white color; strongly bonded with platinum foil
6	1200	30	99.7	4	light gray
7	1200	60	99.9	6	slightly translucent
8	1200	150	99.9	9	translucent
9	1400	30	99.9	18	light gray; glassy appearance
10	1400	60	99.9	20	light cream color; slightly translucent
11	1400	150	99.9	32	white color

Figure 4.024: Hot isostatic pressing densification of BeO (77,79).

Annealing Temperature °C	BeO		
	Modulus of Rupture psi	Standard Deviation psi	Increase in Strength %
Machined	28,200	2,500	—
500	30,700	1,400	9
800	31,900	3,400	13
900	35,400	5,400	26
1,000	35,600	6,100	26
1,100	34,100	4,500	21
1,200	32,400	5,100	15
1,300	—	—	—
1,500	37,600	4,700	33

Figure 4.025-1: Effects of annealing at various temperatures on the strength of machined BeO (86).

Grain Size μm	Modulus of Rupture, psi	
	Machined	Machined then Annealed 1 hr. 1000°C
3.5	24,000	31,700
5.4	24,650	25,500
7.0	23,000	23,000
8.1	20,240	25,275
10.5	19,600	19,400
15.5	17,450	16,740
23.7	17,700	14,650
26.0	14,400	13,100

Figure 4.025-2: Effects of grain size on the strength of machined BeO and BeO annealed after machining (86).